



Journal of Applied and Computational Mechanics



Research Paper

Analysis of Axisymmetric Vibration of Functionally-Graded Circular Nano-Plate Based on the Integral Form of the Strain Gradient Model

Mortaza Pourabdy¹, Mohammad Shishehsaz², Shahram Shahrooi³, S. Alireza S. Roknizadeh⁴

¹ Department of Mechanical Engineering, Ahvaz Branch, Islamic Azad University, Ahvaz, Iran, Email: mortaza-pourabdy@iauahvaz.ir

² Department of Mechanical Engineering, Shahid Chamran University of Ahvaz, Ahvaz, Iran, Email: mshishehsaz@scu.ac.ir

³ Department of Mechanical Engineering, Ahvaz Branch, Islamic Azad University, Ahvaz, Iran, Email: shahramshahrooi@iauahvaz.ac.ir

⁴ Department of Mechanical Engineering, Shahid Chamran University of Ahvaz, Ahvaz, Iran, Email: s.roknizadeh@scu.ac.ir

Received May 18 2021; Revised July 18 2021; Accepted for publication July 21 2021.

Corresponding author: M. Shishehsaz (mshishehsaz@scu.ac.ir)

© 2021 Published by Shahid Chamran University of Ahvaz

Abstract. In this paper, it is aimed to analyze the linear vibrational behavior of functionally-graded (FG) size-dependent circular nano-plates using the integral form of the non-local strain gradient (NSG) model. The linear axisymmetric vibration of the circular FG nano-plates based on the non-local strain gradient (NSG) model is the focal point of this study. In this regard, the non-local elasticity theory (NET) and strain gradient (SG) models are used in conjunction with Hamilton's principle to obtain the governing equations. Discretization of the obtained governing equations is performed with the help of generalized differential quadrature rule (GDQR) and Galerkin weighted residual method (GWRM). The analysis is focused on the effect of non-local and material parameters, as well as the aspect ratio, heterogeneity index of FG material, different boundary conditions, and frequency number on the overall behavior of nano-plate. On using the Galerkin method, a system of linear differential equations is obtained and solved to determine the natural linear frequencies and mode shapes. The obtained results are then compared with the existing results in the literature. On using the proposed procedure in this paper, the dynamic behavior of nano-plate under different boundary conditions can be well described. In addition, the existing deficiencies in other non-local theories can be eliminated. The results of this investigation can be considered as a turning point in the improvement of theoretical results for achieving a better prediction of vibrational behavior in nanostructures.

Keywords: Size effect, vibrational response, functionally graded material, circular nanoplate, non-local strain gradient theory.

1. Introduction

Nowadays, several kinds of research have been devoted to the field of nano-structures regarding their excellent characteristics. However, several limitations are encountered in the testing of nano-scaled samples according to the difficulty and expense of the experimental test. Accordingly, suitable mathematical models should be developed for investigations. The conducted modeling approaches in this field can be classified into three classes of peer atomistic mechanics[1, 2], hybrid atomistic-continuum mechanics[3-6], and peer continuum mechanics. The first and second classes suffer from the higher computational cost, which restricts their application in the analysis of large-scale systems. However, the approaches involved in the last class provide acceptable results consistent with the results of former approaches along with lower computational costs. The results reveal the significant effect of size on the mechanical properties; hence, neglecting of this parameter would lead to an improper solution [7, 8].

According to the neglecting of size effect in the classical continuum theories, their applications in the evaluation of micro/nano-scaled structures are not desirable. To alleviate this problem, continuum theories involving size-dependent effects have been developed. For adapting the continuum mechanics procedure in analyzing the micro-/nano-scaled structures, some modifications should be performed to consider the size effect. In this regard, several models have been proposed, among which, one can mention the non-local elasticity theory (NET), Eringen's theory [9-14], strain gradient theory (SGT)[15-17], surface effect elasticity [18-24], couple stress theory (CST), modified CST [25-31], stress-driven theory [32-34] and the non-local strain gradient theory (NSGT) [35-45].

Zarei et al. [46] Analyzed the Buckling and Vibration of Tapered Circular nano-plate subjected to in-plane forces were studied. They considered a linear variation for the plate thickness in the radial direction and used the nonlocal elasticity theory to capture the size-dependent effects. In addition, Raleigh-Ritz and differential transform methods were utilized to obtain the frequency equations, based on the simply supported and clamped boundary conditions. They investigated the effects of nonlocal and taper



parameters, as well as the mode number, on the natural frequency. Their results showed that increasing the taper parameter causes an increase in buckling load and natural frequencies. These effects were more pronounced for nano-plates with clamped boundary conditions. Barretta et al. [37] analyzed the behavior of an axisymmetric circular/ annular nano-plate, using the stress-driven nonlocal integral elasticity and Kirchhoff plate theory. They applied this method to some engineering case studies and compared the associated results with those of the strain gradient model of elasticity generated by Reissner's variational principle. Nonlinear axisymmetric bending of a thin circular plate was analyzed based on strain gradient theory by Li et al. [47]. They proposed a size-dependent nonlinear bending theory for an axisymmetric thin circular plate, using the principle of minimum potential energy. Their formulation was based on the strain gradient theory of Zhou et al. and the von Kármán geometric nonlinearity. They showed that provided the circular plate thickness is much greater than the higher-order material constant, all strain gradient effects can be ignored and the difference in deflections obtained based on these theories is negligible. Luo et al. [48] analyzed the Transverse free vibration of axisymmetric functionally graded circular nanoplates with radial loads based on the nonlocal strain gradient approach and Mindlin plate theory. They solved the resulting equation of motion by the differential quadrature method. They showed that the natural frequencies of the circular nanoplates decrease with an increase in the radial compressive load while increasing with an increase in radial tensile load. Additionally, the first-mode natural frequency reduces to zero under a certain radial compressive load, resulting in dynamic instability. Also, they demonstrated that the strain gradient characteristic parameter has a threshold in their model for functionally graded circular nanoplate. Yang et al. [49] analyzed the effect of the surface material properties on the deflection and natural frequencies of the circular nano-plates based on different boundary conditions. They used Gurtin–Murdoch surface elasticity theory and the first-order shear deformation plate theory to derive the partial differential equation for the axisymmetric bending and free vibration of the circular nanoplate.

Al-Furjan et al. [27] used modified couple stress theory to investigate the vibrational characteristics of a higher-order laminated composite viscoelastic annular micro-plate resting on a viscoelastic foundation, simulated via the Kelvin-Voight model. They studied the effects of the length scale parameter, radius ratio, circumferential and radial mode number, geometry of the laminated layer, and the boundary conditions on the frequency responses of the annular microplate using the generalized differential quadrature method (GDQM) for various boundary conditions.

Several limitations exist in NET and NSGT. In these theories, the stress at one point in the material is affected by the strains at other points. This relationship was determined using a Fredholm-type integral equation, in which the stress was the convolutional output between the elastic strain and a core function dependent on the non-local parameter [9]. In Refs. [35-45], the integral relationship between the stress and strain was converted into a differential equation and solved accordingly. For this transformation, certain conditions must be satisfied. Some researchers have shown that the equivalence between the integral convolutions and the differential formulations (with suitable non-classical boundary conditions) has been assured for the higher-order nonlocal gradient theory [50, 51] and the nonlocal modified gradient theory [52, 53].

Regarding the reviewed literature, this paper evaluates the axisymmetric linear free vibration of a circular nano-plate based on the integral form of the nonlocal strain gradient model. The analysis will focus on the effect of non-local and material parameters, aspect ratio, heterogeneity index of FG material, different B. Cs, and frequency number on the overall behavior of the axisymmetric nano-plate. For this purpose, the integral form of the NET and SG models are combined and used in conjunction with Hamilton's principle to derive the governing equations. The generalized differential quadrature rule (GDQR) and the Galerkin weighted residual method (GWRM) are used to discretize the governing equation. On using the Galerkin method, a set of linear differential equations is obtained and then, the natural linear frequencies and mode shapes are determined by solving the equation set. To the best of the authors' knowledge, the linear vibrational behavior of the FG circular nano-plates is going to be investigated for the first time using the integral form of the non-local SG model. The obtained results confirm the appropriateness of the proposed method in describing the dynamic behaviors of nano-plates under different B. Cs. Moreover, the proposed method can overcome the existing deficiencies of other non-local theories. The obtained results present a turning point for improving the theoretical results to achieve a better prediction of the vibrational behavior of the nanoplates.

2. Classical plate theory: governing equations of the nano-plates

Figure 1 shows a circular nano-plate made of FG material with a combination of ceramic and metal. The dimensions of this nano-plate are h and R representing the thickness and radius, respectively. According to this figure, the governing equations of motion are extracted based on the cylindrical coordinate system.

The mechanical properties of FG nano-plate are defined as in eq. (1) regarding the power law:

$$E(z) = E_c V^n + E_m (1 - V^n) , \rho(z) = \rho_c V^n + \rho_m (1 - V^n) , \nu(z) = \nu_c V^n + \nu_m (1 - V^n). \tag{1}$$

where E, ρ, ν and n represent the elastic modulus, density, Poisson's ratio, and heterogeneity index of the FG material, respectively. Moreover, m and c indices specify the metal and ceramic phases of FG material, respectively. The volume ratio, V , is defined as;

$$V = \frac{2z + h}{2h} , -\frac{h}{2} \leq z \leq +\frac{h}{2} \tag{2}$$

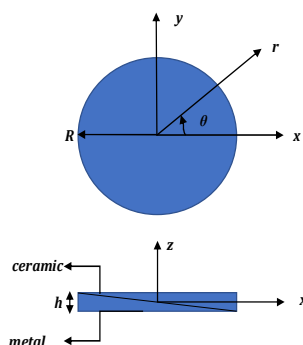


Fig. 1. Geometrical characteristics of the circular nano-plate represented in the cylindrical coordinate system.



Additionally, Poisson's ratio is considered to be constant, as a result of its insignificant variation in the thickness direction. Based on the classical plate theory [54, 55], the components of the displacement field, u_r and u_z , are given as follows:

$$\begin{Bmatrix} u_r(r, z, t) \\ u_z(r, z, t) \end{Bmatrix} = \begin{Bmatrix} u_0(r, t) \\ w_0(r, t) \end{Bmatrix} - z \begin{Bmatrix} \frac{\partial w_0}{\partial r}(r, t) \\ 0 \end{Bmatrix} \tag{3}$$

where, u_0 and w_0 are the displacement functions along the radial and transverse axes of the nano-plate mid-plane, respectively. Also, based on the geometric relations of strain-displacement, non-zero strain components are obtained as follows [54]:

$$\begin{Bmatrix} \varepsilon_{rr} \\ \varepsilon_{\theta\theta} \end{Bmatrix} = \begin{Bmatrix} \varepsilon_{rr}^0 \\ \varepsilon_{\theta\theta}^0 \end{Bmatrix} - z \begin{Bmatrix} \kappa_{rr} \\ \kappa_{\theta\theta} \end{Bmatrix} = \begin{Bmatrix} \frac{\partial u_0}{\partial r} \\ \frac{u_0}{r} \end{Bmatrix} - z \begin{Bmatrix} \frac{\partial^2 w_0}{\partial r^2} \\ \frac{1}{r} \frac{\partial w_0}{\partial r} \end{Bmatrix} \tag{4}$$

where ε_{rr}^0 and $\varepsilon_{\theta\theta}^0$ illustrate the normal strain components of the mid-plane along r and θ axes, respectively. Additionally, κ_{rr} and $\kappa_{\theta\theta}$ are the curvatures of the nano-plate along r and θ .

With the use of Hamilton's principle, the governing motion equations along the radial transverse direction for the BC of circular nano-plate shown in Fig. 1 are extracted as shown in eq. (5-1) and eq. (5-2) [54]:

$$\begin{aligned} \frac{1}{r} \left(\frac{\partial}{\partial r} (rN_{rr}) - N_{\theta\theta} \right) &= I_0 \frac{\partial^2 u_0}{\partial t^2} - I_1 \frac{\partial^2}{\partial t^2} \frac{\partial w_0}{\partial r} \\ \frac{1}{r} \left(\frac{\partial^2}{\partial r^2} (rM_{rr}) - \frac{\partial M_{\theta\theta}}{\partial r} \right) &= I_0 \frac{\partial^2 w_0}{\partial t^2} - I_1 \frac{\partial^2}{\partial t^2} \left(\frac{1}{r} \frac{\partial}{\partial r} (ru_0) \right) - I_2 \frac{\partial^2}{\partial t^2} \left(\frac{1}{r} \frac{\partial}{\partial r} \left(r \frac{\partial w_0}{\partial r} \right) \right) \end{aligned} \tag{5-1}$$

$$N_{rr} = 0 \text{ or } u_0 = 0 \quad , \quad Q_r = 0 \text{ or } w_0 = 0 \quad , \quad M_{rr} = 0 \text{ or } \frac{\partial w_0}{\partial r} = 0. \tag{5-2}$$

In these equations the stress-resultant forces of N_{rr} and $N_{\theta\theta}$, shear force Q_r , as well as the stress resultant moments of M_{rr} and $M_{\theta\theta}$ are defined as follows:

$$\begin{aligned} \begin{Bmatrix} N_{rr} \\ N_{\theta\theta} \end{Bmatrix} &= \int_{-\frac{h}{2}}^{\frac{h}{2}} \begin{Bmatrix} \sigma_{rr} \\ \sigma_{\theta\theta} \end{Bmatrix} dz, \quad \begin{Bmatrix} M_{rr} \\ M_{\theta\theta} \end{Bmatrix} = \int_{-\frac{h}{2}}^{\frac{h}{2}} z \begin{Bmatrix} \sigma_{rr} \\ \sigma_{\theta\theta} \end{Bmatrix} dz, \\ Q_r &= \frac{1}{r} \left(\frac{\partial}{\partial r} (rM_{rr}) - M_{\theta\theta} \right). \end{aligned} \tag{6}$$

In the above relation, σ_{rr} and $\sigma_{\theta\theta}$ denote the components of the stress tensor. In addition, the inertial constants of I_0 , I_1 , and I_2 are represented as:

$$(I_0, I_1, I_2) = \int_{-\frac{h}{2}}^{\frac{h}{2}} (1, z, z^2) \rho dz \tag{7}$$

3. Classical plate theory: The approach of SGT

General formulations of the Toupin–Mindlin strain gradient theory in the orthogonal curvilinear coordinate system are derived in Ref. [56] and are further reduced to cylindrical and spherical coordinates. For the case of an axisymmetric problem, based on the classical plate theory, the non-zero stresses in the cylindrical coordinates are expressed as follows:

$$\begin{aligned} \sigma_{rr} &= \sigma_{rr}^{(0)} - \left\{ \frac{\partial}{\partial r} \sigma_{rr}^{(1)} + \frac{1}{r} (\sigma_{rr}^{(1)} - \sigma_{\theta\theta r}^{(1)} + \sigma_{r\theta\theta}^{(1)}) \right\} \\ \sigma_{\theta\theta} &= \sigma_{\theta\theta}^{(0)} - \left\{ \frac{\partial}{\partial r} \sigma_{r\theta\theta}^{(1)} + \frac{1}{r} (2\sigma_{r\theta\theta}^{(1)} + \sigma_{\theta\theta r}^{(1)}) \right\} \end{aligned} \tag{8}$$

where superscripts (0) and (1) represent the order of stress components in the SG model. These components are defined as:

$$\begin{cases} \sigma_{rr}^{(0)} = E(\varepsilon_{rr} + \nu\varepsilon_{\theta\theta}) \\ \sigma_{\theta\theta}^{(0)} = E(\nu\varepsilon_{rr} + \varepsilon_{\theta\theta}) \end{cases}, \quad \begin{cases} \sigma_{rr}^{(1)} = E\ell_s^2(\varepsilon_{rrr} + \nu\varepsilon_{\theta\theta r}) \\ \sigma_{\theta\theta r}^{(1)} = E\ell_s^2(\nu\varepsilon_{rrr} + \varepsilon_{\theta\theta r}) \\ \sigma_{r\theta\theta}^{(1)} = E\ell_s^2(1 - \nu^2)\varepsilon_{r\theta\theta} \end{cases} \tag{9}$$

in which, ℓ_s illustrates the material size parameter in the SG model. Furthermore, the strain components of the (0) and (1) order are defined as in eq. (10).

$$\begin{cases} \varepsilon_{rr} = \frac{\partial u_r}{\partial r} = \frac{\partial u_0}{\partial r} - z \frac{\partial^2 w_0}{\partial r^2}(r, t) \\ \varepsilon_{\theta\theta} = \frac{u_r}{r} = \frac{1}{r} u_0(r, t) - z \frac{1}{r} \frac{\partial w_0}{\partial r}(r, t) \end{cases}, \quad \begin{cases} \varepsilon_{rrr} = \frac{\partial \varepsilon_{rr}}{\partial r} = \frac{\partial^2 u_0}{\partial r^2} - z \frac{\partial^3 w_0}{\partial r^3}(r, t) \\ \varepsilon_{\theta\theta r} = \frac{\partial \varepsilon_{\theta\theta}}{\partial r} = \left(\frac{1}{r} \frac{\partial u_0}{\partial r} - \frac{1}{r^2} u_0(r, t) \right) - z \left(\frac{1}{r} \frac{\partial^2 w_0}{\partial r^2}(r, t) - \frac{1}{r^2} \frac{\partial w_0}{\partial r}(r, t) \right) \\ \varepsilon_{r\theta\theta} = \frac{1}{r} \left(\frac{\partial}{\partial r} (r\varepsilon_{\theta\theta}) - \varepsilon_{\theta\theta} \right) = \left(\frac{1}{r} \frac{\partial u_0}{\partial r} - \frac{1}{r^2} u_0(r, t) \right) - z \left(\frac{1}{r} \frac{\partial^2 w_0}{\partial r^2}(r, t) - \frac{1}{r^2} \frac{\partial w_0}{\partial r}(r, t) \right) \end{cases} \tag{10}$$



Using eq. (4) and eqs. (8-10), the stress-resultant forces of N_{rr} and $N_{\theta\theta}$, shear force Q_r , as well as the stress resultant moments of M_{rr} and $M_{\theta\theta}$ are obtained as:

$$(N_{rr}, M_{rr}) = (A, B) \left\{ \left(\frac{\partial u_0}{\partial r} + \frac{\nu}{r} u_0 \right) - \ell_s^2 \left(\frac{\partial^3 u_0}{\partial r^3} + \frac{1}{r} \frac{\partial^2 u_0}{\partial r^2} - \frac{2}{r^2} \frac{\partial u_0}{\partial r} + \frac{2}{r^3} u_0 \right) \right\} - (B, D) \left\{ \left(\frac{\partial^2 w_0}{\partial r^2} + \frac{\nu}{r} \frac{\partial w_0}{\partial r} \right) - \ell_s^2 \left(\frac{\partial^4 w_0}{\partial r^4} + \frac{1}{r} \frac{\partial^3 w_0}{\partial r^3} - \frac{2}{r^2} \frac{\partial^2 w_0}{\partial r^2} + \frac{2}{r^3} \frac{\partial w_0}{\partial r} \right) \right\}, \tag{11-1}$$

$$(N_{\theta\theta}, M_{\theta\theta}) = (A, B) \left\{ \left(\nu \frac{\partial u_0}{\partial r} + \frac{1}{r} u_0 \right) - \ell_s^2 \left(\frac{1}{r} \frac{\partial^2 u_0}{\partial r^2} + \frac{1}{r^2} \frac{\partial u_0}{\partial r} - \frac{1}{r^3} u_0 \right) \right\} - (B, D) \left\{ \left(\nu \frac{\partial^2 w_0}{\partial r^2} + \frac{1}{r} \frac{\partial w_0}{\partial r} \right) - \ell_s^2 \left(\frac{1}{r} \frac{\partial^3 w_0}{\partial r^3} + \frac{1}{r^2} \frac{\partial^2 w_0}{\partial r^2} - \frac{1}{r^3} \frac{\partial w_0}{\partial r} \right) \right\},$$

$$Q_r = B \left(\frac{\partial^2 u_0}{\partial r^2} + \frac{1}{r} \frac{\partial u_0}{\partial r} - \frac{1}{r^2} u_0 \right) - D \left(\frac{\partial^3 w_0}{\partial r^3} + \frac{1}{r} \frac{\partial^2 w_0}{\partial r^2} - \frac{1}{r^2} \frac{\partial w_0}{\partial r} \right) - B \ell_s^2 \left(\frac{\partial^4 u_0}{\partial r^4} + \frac{2}{r} \frac{\partial^3 u_0}{\partial r^3} - \frac{3}{r^2} \frac{\partial^2 u_0}{\partial r^2} + \frac{3}{r^3} \frac{\partial u_0}{\partial r} - \frac{3}{r^4} u_0 \right) + D \ell_s^2 \left(\frac{\partial^5 w_0}{\partial r^5} + \frac{2}{r} \frac{\partial^4 w_0}{\partial r^4} - \frac{3}{r^2} \frac{\partial^3 w_0}{\partial r^3} + \frac{3}{r^3} \frac{\partial^2 w_0}{\partial r^2} - \frac{3}{r^4} \frac{\partial w_0}{\partial r} \right) = 0. \tag{11-2}$$

where the parameters (A, B, D) are the elastic constants of the circular nano-plate and are expressed as:

$$(A, B, D) = \int_{-h/2}^{+h/2} \frac{E(z)}{1-\nu^2} (1, z, z^2) dz \tag{12}$$

Substituting eq. (11) in eq. (5-1), the governing equations of motion for circular nano-plate based on the SG model are given in eqs. (13-1) and (13-2) as:

$$A \left(\frac{\partial^2 u_0}{\partial r^2} + \frac{1}{r} \frac{\partial u_0}{\partial r} - \frac{1}{r^2} u_0 \right) + B \left(\frac{\partial^3 w_0}{\partial r^3} + \frac{1}{r} \frac{\partial^2 w_0}{\partial r^2} - \frac{1}{r^2} \frac{\partial w_0}{\partial r} \right) - A \ell_s^2 \left(\frac{\partial^4 u_0}{\partial r^4} + \frac{2}{r} \frac{\partial^3 u_0}{\partial r^3} - \frac{3}{r^2} \frac{\partial^2 u_0}{\partial r^2} + \frac{3}{r^3} \frac{\partial u_0}{\partial r} - \frac{3}{r^4} u_0 \right) - B \ell_s^2 \left(\frac{\partial^5 w_0}{\partial r^5} + \frac{2}{r} \frac{\partial^4 w_0}{\partial r^4} - \frac{3}{r^2} \frac{\partial^3 w_0}{\partial r^3} + \frac{3}{r^3} \frac{\partial^2 w_0}{\partial r^2} - \frac{3}{r^4} \frac{\partial w_0}{\partial r} \right) = I_0 \frac{\partial^2 u_0}{\partial t^2} - I_1 \frac{\partial}{\partial r} \frac{\partial^2 w_0}{\partial t^2}, \tag{13-1}$$

$$B \left(\frac{\partial^3 u_0}{\partial r^3} + \frac{2}{r} \frac{\partial^2 u_0}{\partial r^2} - \frac{1}{r^2} \frac{\partial u_0}{\partial r} + \frac{1}{r^3} u_0 \right) + D \left(\frac{\partial^4 w_0}{\partial r^4} + \frac{2}{r} \frac{\partial^3 w_0}{\partial r^3} - \frac{1}{r^2} \frac{\partial^2 w_0}{\partial r^2} + \frac{1}{r^3} \frac{\partial w_0}{\partial r} \right) - B \ell_s^2 \left(\frac{\partial^5 u_0}{\partial r^5} + \frac{3}{r} \frac{\partial^4 u_0}{\partial r^4} - \frac{3}{r^2} \frac{\partial^3 u_0}{\partial r^3} + \frac{6}{r^3} \frac{\partial^2 u_0}{\partial r^2} - \frac{9}{r^4} \frac{\partial u_0}{\partial r} + \frac{9}{r^5} u_0 \right) - D \ell_s^2 \left(\frac{\partial^6 w_0}{\partial r^6} + \frac{3}{r} \frac{\partial^5 w_0}{\partial r^5} - \frac{3}{r^2} \frac{\partial^4 w_0}{\partial r^4} + \frac{6}{r^3} \frac{\partial^3 w_0}{\partial r^3} - \frac{9}{r^4} \frac{\partial^2 w_0}{\partial r^2} + \frac{9}{r^5} \frac{\partial w_0}{\partial r} \right) = I_0 \frac{\partial^2 w_0}{\partial t^2} - I_1 \left(\frac{1}{r} \frac{\partial}{\partial r} \left(r \frac{\partial^2 u_0}{\partial t^2} \right) \right) - I_2 \left(\frac{1}{r} \frac{\partial}{\partial r} \left(r \frac{\partial}{\partial r} \frac{\partial^2 w_0}{\partial t^2} \right) \right). \tag{13-2}$$

According to the geometric compatibility conditions, the high-order BCs for the center of nano-plate, $r = 0$, are defined as follows [37]:

$$\ell_s^2 \left(A \frac{\partial^2 u_0}{\partial r^2} - B \frac{\partial^3 w_0}{\partial r^3} \right) = 0 \quad , \quad \ell_s^2 \left(B \frac{\partial^2 u_0}{\partial r^2} - D \frac{\partial^3 w_0}{\partial r^3} \right) = 0. \tag{14}$$

also, the high-order BCs for the edge of the Nano-plate, $r = R$, are defined as follows [37]:

$$A \ell_s^2 \left(\frac{\partial^2 u_0}{\partial r^2} + \nu \left(\frac{1}{r} \frac{\partial u_0}{\partial r} - \frac{1}{r^2} u_0 \right) \right) - B \ell_s^2 \left(\frac{\partial^3 w_0}{\partial r^3} + \nu \left(\frac{1}{r} \frac{\partial^2 w_0}{\partial r^2} - \frac{1}{r^2} \frac{\partial w_0}{\partial r} \right) \right) = 0, \tag{15}$$

$$B \ell_s^2 \left(\frac{\partial^2 u_0}{\partial r^2} + \nu \left(\frac{1}{r} \frac{\partial u_0}{\partial r} - \frac{1}{r^2} u_0 \right) \right) - D \ell_s^2 \left(\frac{\partial^3 w_0}{\partial r^3} + \nu \left(\frac{1}{r} \frac{\partial^2 w_0}{\partial r^2} - \frac{1}{r^2} \frac{\partial w_0}{\partial r} \right) \right) = 0.$$

Based on eqs. (5-2) and (11), the BCs of nano-plate are also derived and shown in Table 1.



Table 1. The considered BCs in SG model.

Boundary type	Boundary condition
Center of plate	$u_0 = \frac{dw_0}{dr} = 0,$ $Q_r = 0 \Rightarrow B \left(\frac{\partial^2 u_0}{\partial r^2} - \ell_s^2 \frac{\partial^4 u_0}{\partial r^4} \right) - D \left(\frac{\partial^3 w_0}{\partial r^3} - \ell_s^2 \frac{\partial^5 w_0}{\partial r^5} \right) = 0.$
Clamped	$u_0 = w_0 = \frac{dw_0}{dr} = 0$
Simply supported	$u_0 = w_0 = 0,$ $M_r = B \left\{ \left(\frac{\partial u_0}{\partial r} + \frac{\nu}{r} u_0 \right) - \ell_s^2 \left[\frac{\partial^3 u_0}{\partial r^3} + \frac{1}{r} \frac{\partial^2 u_0}{\partial r^2} - \frac{2}{r^2} \frac{\partial u_0}{\partial r} + \frac{2}{r^3} u_0 \right] \right\}$ $- D \left\{ \left(\frac{\partial^2 w_0}{\partial r^2} + \frac{\nu}{r} \frac{\partial w_0}{\partial r} \right) - \ell_s^2 \left(\frac{\partial^4 w_0}{\partial r^4} + \frac{1}{r} \frac{\partial^3 w_0}{\partial r^3} - \frac{2}{r^2} \frac{\partial^2 w_0}{\partial r^2} + \frac{2}{r^3} \frac{\partial w_0}{\partial r} \right) \right\}.$
Free	$N_r = A \left\{ \left(\frac{\partial u_0}{\partial r} + \frac{\nu}{r} u_0 \right) - \ell_s^2 \left(\frac{\partial^3 u_0}{\partial r^3} + \frac{1}{r} \frac{\partial^2 u_0}{\partial r^2} - \frac{2}{r^2} \frac{\partial u_0}{\partial r} + \frac{2}{r^3} u_0 \right) \right\}$ $- B \left\{ \left(\frac{\partial^2 w_0}{\partial r^2} + \frac{\nu}{r} \frac{\partial w_0}{\partial r} \right) - \ell_s^2 \left(\frac{\partial^4 w_0}{\partial r^4} + \frac{1}{r} \frac{\partial^3 w_0}{\partial r^3} - \frac{2}{r^2} \frac{\partial^2 w_0}{\partial r^2} + \frac{2}{r^3} \frac{\partial w_0}{\partial r} \right) \right\} = 0,$ $Q_r = B \left(\frac{\partial^2 u_0}{\partial r^2} + \frac{1}{r} \frac{\partial u_0}{\partial r} - \frac{1}{r^2} u_0 \right) - D \left(\frac{\partial^3 w_0}{\partial r^3} + \frac{1}{r} \frac{\partial^2 w_0}{\partial r^2} - \frac{1}{r^2} \frac{\partial w_0}{\partial r} \right)$ $- B \ell_s^2 \left(\frac{\partial^4 u_0}{\partial r^4} + \frac{2}{r} \frac{\partial^3 u_0}{\partial r^3} - \frac{3}{r^2} \frac{\partial^2 u_0}{\partial r^2} + \frac{3}{r^3} \frac{\partial u_0}{\partial r} - \frac{3}{r^4} u_0 \right)$ $+ D \ell_s^2 \left(\frac{\partial^5 w_0}{\partial r^5} + \frac{2}{r} \frac{\partial^4 w_0}{\partial r^4} - \frac{3}{r^2} \frac{\partial^3 w_0}{\partial r^3} + \frac{3}{r^3} \frac{\partial^2 w_0}{\partial r^2} - \frac{3}{r^4} \frac{\partial w_0}{\partial r} \right) = 0,$ $M_r = B \left\{ \left(\frac{\partial u_0}{\partial r} + \frac{\nu}{r} u_0 \right) - \ell_s^2 \left[\frac{\partial^3 u_0}{\partial r^3} + \frac{1}{r} \frac{\partial^2 u_0}{\partial r^2} - \frac{2}{r^2} \frac{\partial u_0}{\partial r} + \frac{2}{r^3} u_0 \right] \right\}$ $- D \left\{ \left(\frac{\partial^2 w_0}{\partial r^2} + \frac{\nu}{r} \frac{\partial w_0}{\partial r} \right) - \ell_s^2 \left(\frac{\partial^4 w_0}{\partial r^4} + \frac{1}{r} \frac{\partial^3 w_0}{\partial r^3} - \frac{2}{r^2} \frac{\partial^2 w_0}{\partial r^2} + \frac{2}{r^3} \frac{\partial w_0}{\partial r} \right) \right\} = 0.$

4. Classical plate theory: The approach of NSGT

According to the NSG model along with the assumptions of classical plate theory, the non-zero stresses in the cylindrical coordinate system are defined as follows:

$$\begin{Bmatrix} \sigma_{rr}^{(0)} \\ \sigma_{\theta\theta}^{(0)} \end{Bmatrix} = E(z) \int_0^R \varphi_{e\alpha} \begin{Bmatrix} \varepsilon_{rr} + \nu \varepsilon_{\theta\theta} \\ \nu \varepsilon_{rr} + \varepsilon_{\theta\theta} \end{Bmatrix} d\rho \tag{16}$$

$$\begin{Bmatrix} \sigma_{rr}^{(1)} \\ \sigma_{\theta\theta}^{(1)} \end{Bmatrix} = \ell_s^2 E(z) \int_0^R \varphi_{e\alpha} \begin{Bmatrix} \varepsilon_{rrr} + \nu \varepsilon_{\theta\theta r} \\ \nu \varepsilon_{rrr} + \varepsilon_{\theta\theta r} \end{Bmatrix} d\rho, \quad \sigma_{r\theta\theta}^{(1)} = \ell_s^2 E(z) (1 - \nu^2) \int_0^R \varphi_{e\alpha} \varepsilon_{r\theta\theta} d\rho$$

where $\varphi_{e\alpha}$ is a kernel function with the conditions shown in eq. (17):

$$\varphi_{e\alpha}(r) \geq 0, \quad \int_{-\infty}^{+\infty} \varphi_{e\alpha}(r) dr = 1, \quad \lim_{e\alpha \rightarrow 0^+} \int_{-\infty}^{+\infty} \varphi_{e\alpha}(r - \rho) f(\rho) d\rho = f(\rho). \tag{17}$$

moreover, in eq. (17), $e\alpha$ is the non-local size parameter in the NSG model and f can be any continuous function [37].

Using eq. (4), (10) and eq. (16), the resultant stress based on the NSG model is determined as:

$$\begin{aligned} N_r &= A \int_0^R \varphi_{e\alpha}(r, \rho) \left\{ \left(\frac{\partial u_0}{\partial \rho} + \frac{\nu}{\rho} u_0 \right) - \ell_s^2 \left(\frac{\partial^3 u_0}{\partial \rho^3} + \frac{1}{\rho} \frac{\partial^2 u_0}{\partial \rho^2} - \frac{2}{\rho^2} \frac{\partial u_0}{\partial \rho} + \frac{2}{\rho^3} u_0 \right) \right\} d\rho \\ &\quad - B \int_0^R \varphi_{e\alpha}(r, \rho) \left\{ \left(\frac{\partial^2 w_0}{\partial \rho^2} + \frac{\nu}{\rho} \frac{\partial w_0}{\partial \rho} \right) - \ell_s^2 \left(\frac{\partial^4 w_0}{\partial \rho^4} + \frac{1}{\rho} \frac{\partial^3 w_0}{\partial \rho^3} - \frac{2}{\rho^2} \frac{\partial^2 w_0}{\partial \rho^2} + \frac{2}{\rho^3} \frac{\partial w_0}{\partial \rho} \right) \right\} d\rho \\ N_{\theta\theta} &= A \int_0^R \varphi_{e\alpha}(r, \rho) \left\{ \left(\nu \frac{\partial u_0}{\partial \rho} + \frac{1}{\rho} u_0 \right) - \ell_s^2 \left(\frac{1}{\rho} \frac{\partial^2 u_0}{\partial \rho^2} + \frac{1}{\rho^2} \frac{\partial u_0}{\partial \rho} - \frac{1}{\rho^3} u_0 \right) \right\} d\rho \\ &\quad - B \int_0^R \varphi_{e\alpha}(r, \rho) \left\{ \left(\nu \frac{\partial^2 w_0}{\partial \rho^2} + \frac{1}{\rho} \frac{\partial w_0}{\partial \rho} \right) - \ell_s^2 \left(\frac{1}{\rho} \frac{\partial^3 w_0}{\partial \rho^3} + \frac{1}{\rho^2} \frac{\partial^2 w_0}{\partial \rho^2} - \frac{1}{\rho^3} \frac{\partial w_0}{\partial \rho} \right) \right\} d\rho \end{aligned} \tag{18-1}$$



$$\begin{aligned}
 M_{rr} &= B \int_0^R \varphi_{e,a}(r, \rho) \left\{ \left(\frac{\partial u_0}{\partial \rho} + \frac{\nu}{\rho} u_0 \right) - \ell_s^2 \left(\frac{\partial^3 u_0}{\partial \rho^3} + \frac{1}{\rho} \frac{\partial^2 u_0}{\partial \rho^2} - \frac{2}{\rho^2} \frac{\partial u_0}{\partial \rho} + \frac{2}{\rho^3} u_0 \right) \right\} d\rho \\
 &\quad - D \int_0^R \varphi_{e,a}(r, \rho) \left\{ \left(\frac{\partial^2 w_0}{\partial \rho^2} + \frac{\nu}{\rho} \frac{\partial w_0}{\partial \rho} \right) - \ell_s^2 \left(\frac{\partial^4 w_0}{\partial \rho^4} + \frac{1}{\rho} \frac{\partial^3 w_0}{\partial \rho^3} - \frac{2}{\rho^2} \frac{\partial^2 w_0}{\partial \rho^2} + \frac{2}{\rho^3} \frac{\partial w_0}{\partial \rho} \right) \right\} d\rho \\
 M_{\theta\theta} &= B \int_0^R \varphi_{e,a}(r, \rho) \left\{ \left(\nu \frac{\partial u_0}{\partial \rho} + \frac{1}{\rho} u_0 \right) - \ell_s^2 \left(\frac{1}{\rho} \frac{\partial^2 u_0}{\partial \rho^2} + \frac{1}{\rho^2} \frac{\partial u_0}{\partial \rho} - \frac{1}{\rho^3} u_0 \right) \right\} d\rho \\
 &\quad - D \int_0^R \varphi_{e,a}(r, \rho) \left\{ \left(\nu \frac{\partial^2 w_0}{\partial \rho^2} + \frac{1}{\rho} \frac{\partial w_0}{\partial \rho} \right) - \ell_s^2 \left(\frac{1}{\rho} \frac{\partial^3 w_0}{\partial \rho^3} + \frac{1}{\rho^2} \frac{\partial^2 w_0}{\partial \rho^2} - \frac{1}{\rho^3} \frac{\partial w_0}{\partial \rho} \right) \right\} d\rho
 \end{aligned} \tag{18-2}$$

Substituting eq. (18-1) and (18-2) in eq. (5-1), the governing equations of motion for circular nano-plate based on the NSG model are obtained as:

$$\begin{aligned}
 &\frac{1}{r} \frac{\partial}{\partial r} \left\{ A r \int_0^R \varphi_{e,a}(r, \rho) \left\{ \left(\frac{\partial u_0}{\partial \rho} + \frac{\nu}{\rho} u_0 \right) - \ell_s^2 \left(\frac{\partial^3 u_0}{\partial \rho^3} + \frac{1}{\rho} \frac{\partial^2 u_0}{\partial \rho^2} - \frac{2}{\rho^2} \frac{\partial u_0}{\partial \rho} + \frac{2}{\rho^3} u_0 \right) \right\} d\rho \right. \\
 &\quad \left. - B r \int_0^R \varphi_{e,a}(r, \rho) \left\{ \left(\frac{\partial^2 w_0}{\partial \rho^2} + \frac{\nu}{\rho} \frac{\partial w_0}{\partial \rho} \right) - \ell_s^2 \left(\frac{\partial^4 w_0}{\partial \rho^4} + \frac{1}{\rho} \frac{\partial^3 w_0}{\partial \rho^3} - \frac{2}{\rho^2} \frac{\partial^2 w_0}{\partial \rho^2} + \frac{2}{\rho^3} \frac{\partial w_0}{\partial \rho} \right) \right\} d\rho \right\} \\
 &- \frac{1}{r} \left\{ A \int_0^R \varphi_{e,a}(r, \rho) \left\{ \left(\nu \frac{\partial u_0}{\partial \rho} + \frac{1}{\rho} u_0 \right) - \ell_s^2 \left(\frac{1}{\rho} \frac{\partial^2 u_0}{\partial \rho^2} + \frac{1}{\rho^2} \frac{\partial u_0}{\partial \rho} - \frac{1}{\rho^3} u_0 \right) \right\} d\rho \right. \\
 &\quad \left. - B \int_0^R \varphi_{e,a}(r, \rho) \left\{ \left(\frac{\partial^2 w_0}{\partial \rho^2} + \frac{\nu}{\rho} \frac{\partial w_0}{\partial \rho} \right) - \ell_s^2 \left(\frac{1}{\rho} \frac{\partial^3 w_0}{\partial \rho^3} + \frac{1}{\rho^2} \frac{\partial^2 w_0}{\partial \rho^2} - \frac{1}{\rho^3} \frac{\partial w_0}{\partial \rho} \right) \right\} d\rho \right\} = I_0 \frac{\partial^2 u_0}{\partial t^2} - I_1 \frac{\partial}{\partial r} \frac{\partial^2 w_0}{\partial t^2}
 \end{aligned} \tag{19-1}$$

$$\begin{aligned}
 &\frac{1}{r} \frac{\partial^2}{\partial r^2} \left\{ r B \int_0^R \varphi_{e,a}(r, \rho) \left\{ \left(\frac{\partial u_0}{\partial \rho} + \frac{\nu}{\rho} u_0 \right) - \ell_s^2 \left(\frac{\partial^3 u_0}{\partial \rho^3} + \frac{1}{\rho} \frac{\partial^2 u_0}{\partial \rho^2} - \frac{2}{\rho^2} \frac{\partial u_0}{\partial \rho} + \frac{2}{\rho^3} u_0 \right) \right\} d\rho \right. \\
 &\quad \left. - r D \int_0^R \varphi_{e,a}(r, \rho) \left\{ \left(\frac{\partial^2 w_0}{\partial \rho^2} + \frac{\nu}{\rho} \frac{\partial w_0}{\partial \rho} \right) - \ell_s^2 \left(\frac{\partial^4 w_0}{\partial \rho^4} + \frac{1}{\rho} \frac{\partial^3 w_0}{\partial \rho^3} - \frac{2}{\rho^2} \frac{\partial^2 w_0}{\partial \rho^2} + \frac{2}{\rho^3} \frac{\partial w_0}{\partial \rho} \right) \right\} d\rho \right\} \\
 &- \frac{1}{r} \frac{\partial}{\partial r} \left\{ B \int_0^R \varphi_{e,a}(r, \rho) \left\{ \left(\nu \frac{\partial u_0}{\partial \rho} + \frac{1}{\rho} u_0 \right) - \ell_s^2 \left(\frac{1}{\rho} \frac{\partial^2 u_0}{\partial \rho^2} + \frac{1}{\rho^2} \frac{\partial u_0}{\partial \rho} - \frac{1}{\rho^3} u_0 \right) \right\} d\rho \right. \\
 &\quad \left. - D \int_0^R \varphi_{e,a}(r, \rho) \left\{ \left(\frac{\partial^2 w_0}{\partial \rho^2} + \frac{\nu}{\rho} \frac{\partial w_0}{\partial \rho} \right) - \ell_s^2 \left(\frac{1}{\rho} \frac{\partial^3 w_0}{\partial \rho^3} + \frac{1}{\rho^2} \frac{\partial^2 w_0}{\partial \rho^2} - \frac{1}{\rho^3} \frac{\partial w_0}{\partial \rho} \right) \right\} d\rho \right\} \\
 &= I_0 \frac{\partial^2 w_0}{\partial t^2} - I_1 \left(\frac{1}{r} \frac{\partial}{\partial r} \left(r \frac{\partial^2 u_0}{\partial t^2} \right) \right) - I_2 \left(\frac{1}{r} \frac{\partial}{\partial r} \left(r \frac{\partial}{\partial r} \frac{\partial^2 w_0}{\partial t^2} \right) \right)
 \end{aligned} \tag{19-2}$$

Based on eq. (5-2), (18-1) and (18-2), the BCs of the nano-plate are also derived and shown in Table 2. According to the geometric compatibility conditions, the high-order BCs at the nano-plate center ($r = 0$), are defined as:

$$\ell_s^2 \int_0^R \varphi_{e,a}(r, \rho) \left(A \frac{\partial^2 u_0}{\partial \rho^2} - B \frac{\partial^3 w_0}{\partial \rho^3} \right) d\rho = 0 \quad , \quad \ell_s^2 \int_0^R \varphi_{e,a}(r, \rho) \left(B \frac{\partial^2 u_0}{\partial \rho^2} - D \frac{\partial^3 w_0}{\partial \rho^3} \right) d\rho = 0 \tag{20}$$

In addition, the high-order BCs for the edge of nano-plate, $r = R$, are defined as:

$$\begin{cases} A \ell_s^2 \int_0^R \varphi_{e,a}(r, \rho) \left(\frac{\partial^2 u_0}{\partial \rho^2} + \nu \left(\frac{1}{\rho} \frac{\partial u_0}{\partial \rho} - \frac{1}{\rho^2} u_0 \right) \right) d\rho - B \ell_s^2 \int_0^R \varphi_{e,a}(r, \rho) \left(\frac{\partial^3 w_0}{\partial \rho^3} + \nu \left(\frac{1}{\rho} \frac{\partial^2 w_0}{\partial \rho^2} - \frac{1}{\rho^2} \frac{\partial w_0}{\partial \rho} \right) \right) d\rho = 0 \\ B \ell_s^2 \int_0^R \varphi_{e,a}(r, \rho) \left(\frac{\partial^2 u_0}{\partial \rho^2} + \nu \left(\frac{1}{\rho} \frac{\partial u_0}{\partial \rho} - \frac{1}{\rho^2} u_0 \right) \right) d\rho - D \ell_s^2 \int_0^R \varphi_{e,a}(r, \rho) \left(\frac{\partial^3 w_0}{\partial \rho^3} + \nu \left(\frac{1}{\rho} \frac{\partial^2 w_0}{\partial \rho^2} - \frac{1}{\rho^2} \frac{\partial w_0}{\partial \rho} \right) \right) d\rho = 0 \end{cases} \quad @ r = R. \tag{21}$$

5. Equations of motion in the frequency space

Different solution methodology exists in the literature to deal with the governing equations wherein the kinetic or the kinematic field variables are assumed to have a series solution. In the present study, the problem is formulated in terms of kinematic variables. Faghidian [57] developed a smoothed inverse eigenstrain method to reconstruct the residual field from the limited strain measurements, for three case studies in which the residual stresses were introduced by inelastic beam bending, laser-forming, and shot peening. He showed that the smoothed inverse eigenstrain approach allows suppressing the fluctuations that are contrary to the physics of the problem and can minimize the deviation of measurements from its approximations and also will result in an inverse solution satisfying a full range of continuum mechanics requirements. Faghidian [58] used a modified stress function to developed the reconstruction of the residual stress and eigenstrain fields for three experimental case studies wherein the residual stresses were introduced by the surface peening and showed that the smooth reconstructed residual fields can minimize the deviation of the measurements from its approximation and satisfy all continuum mechanics requirements. However, the Newton iterative method can also be used and as shown in the reference, it has an excellent fast convergence for the regularization parameter while effectively reduces the computational cost.



Table 2. Used BCs in the NSG model.

Boundary type	Boundary condition
Center of plate	$u_0 = \frac{dw_0}{dr} = 0$ $Q_r = 0 \Rightarrow \int_0^R \varphi_{e,a}(r, \rho) \left\{ B \left(\frac{\partial^2 u_0}{\partial \rho^2} - \ell_s^2 \frac{\partial^4 u_0}{\partial \rho^4} \right) - D \left(\frac{\partial^3 w_0}{\partial \rho^3} - \ell_s^2 \frac{\partial^5 w_0}{\partial \rho^5} \right) \right\} d\rho = 0.$
Clamped	$u_0 = w_0 = \frac{dw_0}{dr} = 0$
Simply supported	$u_0 = w_0 = 0$ $M_{rr} = 0 \Rightarrow B \int_0^R \varphi_{e,a}(r, \rho) \left\{ \left(\frac{\partial u_0}{\partial \rho} + \frac{\nu}{\rho} u_0 \right) - \ell_s^2 \left(\frac{\partial^3 u_0}{\partial \rho^3} + \frac{1}{\rho} \frac{\partial^2 u_0}{\partial \rho^2} - \frac{2}{\rho^2} \frac{\partial u_0}{\partial \rho} + \frac{2}{\rho^3} u_0 \right) \right\} d\rho$ $- D \int_0^R \varphi_{e,a}(r, \rho) \left\{ \left(\frac{\partial^2 w_0}{\partial \rho^2} + \frac{\nu}{\rho} \frac{\partial w_0}{\partial \rho} \right) - \ell_s^2 \left(\frac{\partial^4 w_0}{\partial \rho^4} + \frac{1}{\rho} \frac{\partial^3 w_0}{\partial \rho^3} - \frac{2}{\rho^2} \frac{\partial^2 w_0}{\partial \rho^2} + \frac{2}{\rho^3} \frac{\partial w_0}{\partial \rho} \right) \right\} d\rho = 0.$
Free	$N_{rr} = 0 \Rightarrow A \int_0^R \varphi_{e,a}(r, \rho) \left\{ \left(\frac{\partial u_0}{\partial \rho} + \frac{\nu}{\rho} u_0 \right) - \ell_s^2 \left(\frac{\partial^3 u_0}{\partial \rho^3} + \frac{1}{\rho} \frac{\partial^2 u_0}{\partial \rho^2} - \frac{2}{\rho^2} \frac{\partial u_0}{\partial \rho} + \frac{2}{\rho^3} u_0 \right) \right\} d\rho$ $- B \int_0^R \varphi_{e,a}(r, \rho) \left\{ \left(\frac{\partial^2 w_0}{\partial \rho^2} + \frac{\nu}{\rho} \frac{\partial w_0}{\partial \rho} \right) - \ell_s^2 \left(\frac{\partial^4 w_0}{\partial \rho^4} + \frac{1}{\rho} \frac{\partial^3 w_0}{\partial \rho^3} - \frac{2}{\rho^2} \frac{\partial^2 w_0}{\partial \rho^2} + \frac{2}{\rho^3} \frac{\partial w_0}{\partial \rho} \right) \right\} d\rho = 0,$ $Q_r = 0 \Rightarrow \int_0^R \varphi_{e,a}(r, \rho) \left\{ B \left(\frac{\partial^2 u_0}{\partial \rho^2} + \frac{1}{\rho} \frac{\partial u_0}{\partial \rho} - \frac{1}{\rho^2} u_0 \right) - D \left(\frac{\partial^3 w_0}{\partial \rho^3} + \frac{1}{\rho} \frac{\partial^2 w_0}{\partial \rho^2} - \frac{1}{\rho^2} \frac{\partial w_0}{\partial \rho} \right) \right\} d\rho$ $- B \ell_s^2 \int_0^R \varphi_{e,a}(r, \rho) \left(\frac{\partial^4 u_0}{\partial \rho^4} + \frac{2}{\rho} \frac{\partial^3 u_0}{\partial \rho^3} - \frac{3}{\rho^2} \frac{\partial^2 u_0}{\partial \rho^2} + \frac{3}{\rho^3} \frac{\partial u_0}{\partial \rho} - \frac{3}{\rho^4} u_0 \right) d\rho$ $+ D \ell_s^2 \int_0^R \varphi_{e,a}(r, \rho) \left(\frac{\partial^5 w_0}{\partial \rho^5} + \frac{2}{\rho} \frac{\partial^4 w_0}{\partial \rho^4} - \frac{3}{\rho^2} \frac{\partial^3 w_0}{\partial \rho^3} + \frac{3}{\rho^3} \frac{\partial^2 w_0}{\partial \rho^2} - \frac{3}{\rho^4} \frac{\partial w_0}{\partial \rho} \right) d\rho = 0,$ $M_{rr} = 0 \Rightarrow B \int_0^R \varphi_{e,a}(r, \rho) \left\{ \left(\frac{\partial u_0}{\partial \rho} + \frac{\nu}{\rho} u_0 \right) - \ell_s^2 \left(\frac{\partial^3 u_0}{\partial \rho^3} + \frac{1}{\rho} \frac{\partial^2 u_0}{\partial \rho^2} - \frac{2}{\rho^2} \frac{\partial u_0}{\partial \rho} + \frac{2}{\rho^3} u_0 \right) \right\} d\rho$ $- D \int_0^R \varphi_{e,a}(r, \rho) \left\{ \left(\frac{\partial^2 w_0}{\partial \rho^2} + \frac{\nu}{\rho} \frac{\partial w_0}{\partial \rho} \right) - \ell_s^2 \left(\frac{\partial^4 w_0}{\partial \rho^4} + \frac{1}{\rho} \frac{\partial^3 w_0}{\partial \rho^3} - \frac{2}{\rho^2} \frac{\partial^2 w_0}{\partial \rho^2} + \frac{2}{\rho^3} \frac{\partial w_0}{\partial \rho} \right) \right\} d\rho = 0.$

To investigate the free vibrational behavior of the nano-plate, the oscillating motion assumption is considered for discretizing the equations of motion. Using this assumption, the solution of equations of motion is assumed to be in the form of:

$$\{ u_0(r, t) \quad w_0(r, t) \} = \{ u(r, t) \quad w(r, t) \} e^{i\omega_n t} \tag{22}$$

where ω_n represents the natural frequency for a circular nano-plate.

In the following, the governing equations of circular nano-plate, BCs, and high-order BCs are extracted based on the SG and NSG models.

5.1. Derivation of equations for the nano-plate based on the SG model

Using eq. (22) the equations of motion defined in eqs. (13-1) and (13-2) can be represented as follows:

$$A \left(\frac{d^2 u}{dr^2} + \frac{1}{r} \frac{du}{dr} - \frac{1}{r^2} u \right) + B \left(\frac{d^2 w}{dr^2} + \frac{1}{r} \frac{dw}{dr} - \frac{1}{r^2} w \right) - A \ell_s^2 \left(\frac{d^4 u}{dr^4} + \frac{2}{r} \frac{d^3 u}{dr^3} - \frac{3}{r^2} \frac{d^2 u}{dr^2} + \frac{3}{r^3} \frac{du}{dr} - \frac{3}{r^4} u \right) - B \ell_s^2 \left(\frac{d^5 w}{dr^5} + \frac{2}{r} \frac{d^4 w}{dr^4} - \frac{3}{r^2} \frac{d^3 w}{dr^3} + \frac{3}{r^3} \frac{d^2 w}{dr^2} - \frac{3}{r^4} \frac{dw}{dr} \right) = \left(I_1 \frac{dw}{dr} - I_0 u \right) \omega_n^2 \tag{23-1}$$

$$B \left(\frac{d^3 u}{dr^3} + \frac{2}{r} \frac{d^2 u}{dr^2} - \frac{1}{r^2} \frac{du}{dr} + \frac{1}{r^3} u \right) + D \left(\frac{d^4 w}{dr^4} + \frac{2}{r} \frac{d^3 w}{dr^3} - \frac{1}{r^2} \frac{d^2 w}{dr^2} + \frac{1}{r^3} \frac{dw}{dr} \right) - B \ell_s^2 \left(\frac{d^5 u}{dr^5} + \frac{3}{r} \frac{d^4 u}{dr^4} - \frac{3}{r^2} \frac{d^3 u}{dr^3} + \frac{6}{r^3} \frac{d^2 u}{dr^2} - \frac{9}{r^4} \frac{du}{dr} + \frac{9}{r^5} u \right) - D \ell_s^2 \left(\frac{d^6 w}{dr^6} + \frac{3}{r} \frac{d^5 w}{dr^5} - \frac{3}{r^2} \frac{d^4 w}{dr^4} + \frac{6}{r^3} \frac{d^3 w}{dr^3} - \frac{9}{r^4} \frac{d^2 w}{dr^2} + \frac{9}{r^5} \frac{dw}{dr} \right) = \left(I_2 \left(\frac{1}{r} \frac{d}{dr} \left(r \frac{dw}{dr} \right) \right) + I_1 \left(\frac{1}{r} \frac{d}{dr} (ru) \right) - I_0 w \right) \omega_n^2 \tag{23-2}$$



Similarly, the high-order BCs, eq. (14-15), are redefined as:

$$\ell_s^2 \left(A \frac{d^2 u}{dr^2} - B \frac{d^3 w}{dr^3} \right) = 0, \quad \ell_s^2 \left(B \frac{d^2 u}{dr^2} - D \frac{d^3 w}{dr^3} \right) = 0 \quad @ r = 0. \tag{24-1}$$

$$\begin{cases} A \ell_s^2 \left(\frac{d^2 u_0}{dr^2} + \nu \left(\frac{1}{r} \frac{du_0}{dr} - \frac{1}{r^2} u_0 \right) \right) - B \ell_s^2 \left(\frac{d^3 w_0}{dr^3} + \nu \left(\frac{1}{r} \frac{d^2 w_0}{dr^2} - \frac{1}{r^2} \frac{dw_0}{dr} \right) \right) = 0 \\ B \ell_s^2 \left(\frac{d^2 u_0}{dr^2} + \nu \left(\frac{1}{r} \frac{du_0}{dr} - \frac{1}{r^2} u_0 \right) \right) - D \ell_s^2 \left(\frac{d^3 w_0}{dr^3} + \nu \left(\frac{1}{r} \frac{d^2 w_0}{dr^2} - \frac{1}{r^2} \frac{dw_0}{dr} \right) \right) = 0 \end{cases} \quad @ r = R. \tag{24-2}$$

To investigate the influential parameters on the natural frequency of the circular nano-plate depicted in Fig. 1, the following dimensionless quantities are introduced:

$$\begin{aligned} (s, U, W, \alpha, \bar{h}, L_c) &= \frac{1}{R} (r, u, w, a, h, \ell_s), \\ (\bar{A}, \bar{B}, \bar{D}) &= \left(\frac{AR^2}{D_0}, \frac{BR}{D_0}, \frac{D}{D_0} \right), \quad (\bar{I}_0, \bar{I}_1, \bar{I}_2) = \left(\frac{I_0}{I_{00}}, \frac{I_1}{I_{00}R}, \frac{I_2}{I_{00}R^2} \right). \end{aligned} \tag{25}$$

where

$$D_0 = \frac{E_m h^3}{12(1-\nu^2)}, \quad I_{00} = \rho_m h. \tag{26}$$

Using eq. (25), the equations of motion in the dimensionless form can be described as:

$$\begin{aligned} \bar{A} \left(\frac{d^2 U}{ds^2} + \frac{1}{s} \frac{dU}{ds} - \frac{1}{s^2} U \right) + \bar{B} \left(\frac{d^3 W}{ds^3} + \frac{1}{s} \frac{d^2 W}{ds^2} - \frac{1}{s^2} \frac{dW}{ds} \right) \\ - \bar{A} L_c^2 \left(\frac{d^4 U}{ds^4} + \frac{2}{s} \frac{d^3 U}{ds^3} - \frac{3}{s^2} \frac{d^2 U}{ds^2} + \frac{3}{s^3} \frac{dU}{ds} - \frac{3}{s^4} U \right) \\ - \bar{B} L_c^2 \left(\frac{d^5 W}{ds^5} + \frac{2}{r} \frac{d^4 W}{dr^4} - \frac{3}{r^2} \frac{d^3 W}{dr^3} + \frac{3}{r^3} \frac{d^2 W}{dr^2} - \frac{3}{r^4} \frac{dW}{dr} \right) = \left(\bar{I}_1 \frac{dW}{dr} - \bar{I}_0 U \right) \Omega_n^2 \end{aligned} \tag{27-1}$$

$$\begin{aligned} \bar{B} \left(\frac{d^3 U}{ds^3} + \frac{2}{s} \frac{d^2 U}{ds^2} - \frac{1}{s^2} \frac{dU}{ds} + \frac{1}{s^3} U \right) + \bar{D} \left(\frac{d^4 W}{ds^4} + \frac{2}{s} \frac{d^3 W}{ds^3} - \frac{1}{s^2} \frac{d^2 W}{ds^2} + \frac{1}{s^3} \frac{dW}{ds} \right) \\ - \bar{B} L_c^2 \left(\frac{d^5 U}{ds^5} + \frac{3}{s} \frac{d^4 U}{ds^4} - \frac{3}{s^2} \frac{d^3 U}{ds^3} + \frac{6}{s^3} \frac{d^2 U}{ds^2} - \frac{9}{s^4} \frac{dU}{ds} + \frac{9}{s^5} U \right) \\ - \bar{D} L_c^2 \left(\frac{d^6 W}{ds^6} + \frac{3}{s} \frac{d^5 W}{ds^5} - \frac{3}{s^2} \frac{d^4 W}{ds^4} + \frac{6}{s^3} \frac{d^3 W}{ds^3} - \frac{9}{s^4} \frac{d^2 W}{ds^2} + \frac{9}{s^5} \frac{dW}{ds} \right) \\ = \left(\bar{I}_2 \left(\frac{1}{s} \frac{d}{ds} \left(s \frac{dW}{ds} \right) \right) + \bar{I}_1 \left(\frac{1}{s} \frac{d}{ds} (sU) \right) - \bar{I}_0 W \right) \Omega_n^2 \end{aligned} \tag{27-2}$$

where Ω_n is the dimensionless natural frequency and is defined as:

$$\Omega_n^2 = \frac{I_0 R^4}{D} \omega_n^2 \tag{28}$$

Furthermore, the high-order BCs, eqs. (24-1) and (24-2), based on eq. (25) are defined as follows:

$$\left\{ L_s^2 \left(\bar{A} \frac{d^2 U}{ds^2} - \bar{B} \frac{d^3 W}{ds^3} \right) = 0, \quad L_s^2 \left(\bar{A} \frac{d^2 U}{ds^2} - \bar{B} \frac{d^3 W}{ds^3} \right) = 0 \quad @ s = 0. \right. \tag{29-1}$$

$$\begin{cases} \bar{A} L_c^2 \left(\frac{d^2 U}{ds^2} + \nu \left(\frac{1}{s} \frac{dU}{ds} - \frac{1}{s^2} U \right) \right) - \bar{B} L_c^2 \left(\frac{d^3 W}{ds^3} + \nu \left(\frac{1}{s} \frac{d^2 W}{ds^2} - \frac{1}{s^2} \frac{dW}{ds} \right) \right) = 0 \\ \bar{B} L_c^2 \left(\frac{d^2 U}{ds^2} + \nu \left(\frac{1}{s} \frac{dU}{ds} - \frac{1}{s^2} U \right) \right) - \bar{D} L_c^2 \left(\frac{d^3 W}{ds^3} + \nu \left(\frac{1}{s} \frac{d^2 W}{ds^2} - \frac{1}{s^2} \frac{dW}{ds} \right) \right) = 0 \end{cases} \quad @ s = 1. \tag{29-2}$$

Likewise, regarding eq. (25), for the boundary conditions introduced in Table 1, the corresponding non-dimensional equations are given in Table 3.

Table 3. Dimensionless BCs based on the SG model in frequency space.

Boundary type	Boundary condition
Center of plate	$U = \frac{dW}{dr} = 0, \quad Q_r = 0 \Rightarrow B \left\{ \frac{d^2 U}{ds^2} - L_c^2 \frac{d^4 U}{ds^4} \right\} - D \left\{ \frac{d^3 W}{ds^3} - L_c^2 \frac{d^5 W}{ds^5} \right\} = 0$



Table 3. Continued.

Clamped	$U = W = \frac{dW}{dr} = 0$
Simply supported	$U = W = 0$ $M_{rr} = 0 \Rightarrow \bar{B} \left\{ \left(\frac{dU}{ds} + \frac{\nu}{s} U \right) - L_c^2 \left[\frac{d^3 U}{ds^3} + \frac{1}{s} \frac{d^2 U}{ds^2} - \frac{2}{s^2} \frac{dU}{ds} + \frac{2}{s^3} U \right] \right\}$ $- \bar{D} \left\{ \left(\frac{d^2 W}{ds^2} + \frac{\nu}{s} \frac{dW}{ds} \right) - L_c^2 \left[\frac{d^4 W}{ds^4} + \frac{1}{s} \frac{d^3 W}{ds^3} - \frac{2}{s^2} \frac{d^2 W}{ds^2} + \frac{2}{s^3} \frac{dW}{ds} \right] \right\} = 0$
Free	$N_{rr} = 0 \Rightarrow \bar{A} \left\{ \left(\frac{dU}{ds} + \frac{\nu}{s} U \right) - L_c^2 \left[\frac{d^3 U}{ds^3} + \frac{1}{s} \frac{d^2 U}{ds^2} - \frac{2}{s^2} \frac{dU}{ds} + \frac{2}{s^3} U \right] \right\}$ $- \bar{B} \left\{ \left(\frac{d^2 W}{ds^2} + \frac{\nu}{s} \frac{dW}{ds} \right) - L_c^2 \left[\frac{d^4 W}{ds^4} + \frac{1}{s} \frac{d^3 W}{ds^3} - \frac{2}{s^2} \frac{d^2 W}{ds^2} + \frac{2}{s^3} \frac{dW}{ds} \right] \right\} = 0,$ $M_{rr} = 0 \Rightarrow \bar{B} \left\{ \left(\frac{dU}{ds} + \frac{\nu}{s} U \right) - L_c^2 \left[\frac{d^3 U}{ds^3} + \frac{1}{s} \frac{d^2 U}{ds^2} - \frac{2}{s^2} \frac{dU}{ds} + \frac{2}{s^3} U \right] \right\}$ $- \bar{D} \left\{ \left(\frac{d^2 W}{ds^2} + \frac{\nu}{s} \frac{dW}{ds} \right) - L_c^2 \left[\frac{d^4 W}{ds^4} + \frac{1}{s} \frac{d^3 W}{ds^3} - \frac{2}{s^2} \frac{d^2 W}{ds^2} + \frac{2}{s^3} \frac{dW}{ds} \right] \right\} = 0,$ $Q_r = 0 \Rightarrow \bar{B} \left(\frac{d^2 U}{ds^2} + \frac{1}{s} \frac{dU}{ds} - \frac{1}{s^2} U \right) - \bar{D} \left(\frac{d^3 W}{ds^3} + \frac{1}{s} \frac{d^2 W}{ds^2} - \frac{1}{s^2} \frac{dW}{ds} \right)$ $- \bar{B} L_c^2 \left(\frac{d^4 U}{ds^4} + \frac{2}{s} \frac{d^3 U}{ds^3} - \frac{3}{s^2} \frac{d^2 U}{ds^2} + \frac{3}{s^3} \frac{dU}{ds} - \frac{3}{s^4} U \right)$ $+ \bar{D} L_c^2 \left(\frac{d^5 W}{ds^5} + \frac{2}{s} \frac{d^4 W}{ds^4} - \frac{3}{s^2} \frac{d^3 W}{ds^3} + \frac{3}{s^3} \frac{d^2 W}{ds^2} - \frac{3}{s^4} \frac{dW}{ds} \right) = 0.$

5.2. Analysis of the nano-plate based on the NSG model

Using eq. (22), the equations of motion defined in eqs. (19-1) and (19-2) are recast as:

$$\begin{aligned} & \frac{1}{r} \frac{\partial}{\partial r} \left\{ A r \int_0^R \varphi_{e,a}(r, \rho) \left[\left(\frac{du}{d\rho} + \frac{\nu}{\rho} u \right) - L_c^2 \left(\frac{\partial^3 u_0}{\partial \rho^3} + \frac{1}{\rho} \frac{\partial^2 u}{\partial \rho^2} - \frac{2}{\rho^2} \frac{\partial u}{\partial \rho} + \frac{2}{\rho^3} u \right) \right] d\rho \right. \\ & \quad - B r \int_0^R \varphi_{e,a}(r, \rho) \left[\left(\frac{d^2 w}{d\rho^2} + \frac{\nu}{\rho} \frac{dw}{d\rho} \right) - L_c^2 \left(\frac{d^4 w}{d\rho^4} + \frac{1}{\rho} \frac{d^3 w}{d\rho^3} - \frac{2}{\rho^2} \frac{d^2 w}{d\rho^2} + \frac{2}{\rho^3} \frac{dw}{d\rho} \right) \right] d\rho \left. \right\} \\ & \quad - \frac{1}{r} \left[A \int_0^R \varphi_{e,a}(r, \rho) \left[\left(\nu \frac{du}{d\rho} + \frac{1}{\rho} u \right) - L_c^2 \left(\frac{1}{\rho} \frac{d^2 u}{d\rho^2} + \frac{1}{\rho^2} \frac{du}{d\rho} - \frac{1}{\rho^3} u \right) \right] d\rho \right. \\ & \quad \left. - \frac{1}{r} B \int_0^R \varphi_{e,a}(r, \rho) \left[\left(\frac{d^2 w}{d\rho^2} + \frac{\nu}{\rho} \frac{dw}{d\rho} \right) - L_c^2 \left(\frac{1}{\rho} \frac{d^3 w}{d\rho^3} + \frac{1}{\rho^2} \frac{d^2 w}{d\rho^2} - \frac{1}{\rho^3} \frac{dw}{d\rho} \right) \right] d\rho \right] = \left(I_1 \frac{dw}{dr} - I_0 u \right) \omega_n^2 \end{aligned} \tag{30-1}$$

$$\begin{aligned} & \frac{1}{r} \frac{\partial^2}{\partial r^2} \left\{ r B \int_0^R \varphi_{e,a}(r, \rho) \left[\left(\frac{du}{d\rho} + \frac{\nu}{\rho} u \right) - L_c^2 \left(\frac{d^3 u}{d\rho^3} + \frac{1}{\rho} \frac{d^2 u}{d\rho^2} - \frac{2}{\rho^2} \frac{du}{d\rho} + \frac{2}{\rho^3} u \right) \right] d\rho \right. \\ & \quad - r D \int_0^R \varphi_{e,a}(r, \rho) \left[\left(\frac{d^2 w}{d\rho^2} + \frac{\nu}{\rho} \frac{dw}{d\rho} \right) - L_c^2 \left(\frac{d^4 w}{d\rho^4} + \frac{1}{\rho} \frac{d^3 w}{d\rho^3} - \frac{2}{\rho^2} \frac{d^2 w}{d\rho^2} + \frac{2}{\rho^3} \frac{dw}{d\rho} \right) \right] d\rho \left. \right\} \\ & \quad - \frac{1}{r} \frac{\partial}{\partial r} \left\{ B \int_0^R \varphi_{e,a}(r, \rho) \left[\left(\nu \frac{du}{d\rho} + \frac{1}{\rho} u \right) - L_c^2 \left(\frac{1}{\rho} \frac{d^2 u}{d\rho^2} + \frac{1}{\rho^2} \frac{du}{d\rho} - \frac{1}{\rho^3} u \right) \right] d\rho \right. \\ & \quad \left. - D \int_0^R \varphi_{e,a}(r, \rho) \left[\left(\frac{d^2 w}{d\rho^2} + \frac{\nu}{\rho} \frac{dw}{d\rho} \right) - L_c^2 \left(\frac{1}{\rho} \frac{d^3 w}{d\rho^3} + \frac{1}{\rho^2} \frac{d^2 w}{d\rho^2} - \frac{1}{\rho^3} \frac{dw}{d\rho} \right) \right] d\rho \right\} = \left(I_2 \left(\frac{1}{r} \frac{d}{dr} \left(r \frac{dw}{dr} \right) \right) + I_1 \left(\frac{1}{r} \frac{d}{dr} (ru) \right) - I_0 w \right) \omega_n^2 \end{aligned} \tag{30-2}$$

Moreover, using eq. (25), the high-order BCs, eqs. (20) and (21), are represented as:

$$L_c^2 \int_0^R \varphi_{e,a}(r, \rho) \left(A \frac{d^2 u}{d\rho^2} - B \frac{d^3 w}{d\rho^3} \right) d\rho = 0 \quad , \quad L_c^2 \int_0^R \varphi_{e,a}(r, \rho) \left(B \frac{d^2 u}{d\rho^2} - D \frac{d^3 w}{d\rho^3} \right) d\rho = 0 \quad @ r = 0 \tag{31-1}$$

$$\left\{ \begin{aligned} & A L_c^2 \int_0^R \varphi_{e,a}(r, \rho) \left(\frac{d^2 u}{d\rho^2} + \nu \left(\frac{1}{r\rho} \frac{du}{d\rho} - \frac{1}{\rho^2} u \right) \right) d\rho \\ & \quad - B L_c^2 \int_0^R \varphi_{e,a}(r, \rho) \left(\frac{d^3 w}{d\rho^3} + \nu \left(\frac{1}{\rho} \frac{d^2 w}{d\rho^2} - \frac{1}{\rho^2} \frac{dw}{d\rho} \right) \right) d\rho = 0 \\ & B L_c^2 \int_0^R \varphi_{e,a}(r, \rho) \left(\frac{d^2 u}{d\rho^2} + \nu \left(\frac{1}{r\rho} \frac{du}{d\rho} - \frac{1}{\rho^2} u \right) \right) d\rho \\ & \quad - D L_c^2 \int_0^R \varphi_{e,a}(r, \rho) \left(\frac{d^3 w}{d\rho^3} + \nu \left(\frac{1}{\rho} \frac{d^2 w}{d\rho^2} - \frac{1}{\rho^2} \frac{dw}{d\rho} \right) \right) d\rho = 0 \end{aligned} \right. \quad @ r = R. \tag{31-2}$$



with the use of dimensionless quantities in eq. (25) and defining the non-local dimensionless parameter $\lambda = e_0 a / R$, eqs. (30-1) and (30-2) are recast as:

$$\begin{aligned} & \frac{1}{s} \frac{d}{ds} \left\{ \bar{A} s \int_0^1 \varphi_\lambda(s, \rho) \left[\left(\frac{dU}{d\rho} + \frac{\nu}{\rho} U \right) - I_c^2 \left(\frac{d^3 U}{d\rho^3} + \frac{1}{\rho} \frac{d^2 U}{d\rho^2} - \frac{2}{\rho^2} \frac{dU}{d\rho} + \frac{2}{\rho^3} U \right) \right] d\rho \right. \\ & \quad \left. - \bar{B} s \int_0^1 \varphi_\lambda(s, \rho) \left[\left(\frac{d^2 W}{d\rho^2} + \frac{\nu}{\rho} \frac{\partial W}{\partial \rho} \right) - I_c^2 \left(\frac{d^4 W}{d\rho^4} + \frac{1}{\rho} \frac{d^3 W}{d\rho^3} - \frac{2}{\rho^2} \frac{d^2 W}{d\rho^2} + \frac{2}{\rho^3} \frac{dW}{d\rho} \right) \right] d\rho \right\} \\ & \quad - \frac{1}{s} \left\{ \bar{A} \int_0^1 \varphi_\lambda(s, \rho) \left[\left(\nu \frac{dU}{d\rho} + \frac{1}{\rho} U \right) - I_c^2 \left(\frac{1}{\rho} \frac{d^2 U}{d\rho^2} + \frac{1}{\rho^2} \frac{dU}{d\rho} - \frac{1}{\rho^3} U \right) \right] d\rho \right. \\ & \quad \left. - \frac{1}{s} \bar{B} \int_0^1 \varphi_\lambda(s, \rho) \left[\left(\frac{d^2 W}{d\rho^2} + \frac{\nu}{\rho} \frac{dW}{d\rho} \right) - I_c^2 \left(\frac{1}{\rho} \frac{d^3 W}{d\rho^3} + \frac{1}{\rho^2} \frac{d^2 W}{d\rho^2} - \frac{1}{\rho^3} \frac{dW}{d\rho} \right) \right] d\rho \right\} = \left(\bar{I}_1 \frac{dW}{ds} - \bar{I}_0 U \right) \Omega_n^2 \end{aligned} \tag{32-1}$$

$$\begin{aligned} & \frac{1}{s} \frac{d^2}{ds^2} \left\{ \bar{B} s \int_0^1 \varphi_\lambda(s, \rho) \left[\left(\frac{du}{d\rho} + \frac{\nu}{\rho} u \right) - I_c^2 \left(\frac{d^3 u}{d\rho^3} + \frac{1}{\rho} \frac{d^2 u}{d\rho^2} - \frac{2}{\rho^2} \frac{du}{d\rho} + \frac{2}{\rho^3} u \right) \right] d\rho \right. \\ & \quad \left. - \bar{D} s \int_0^1 \varphi_\lambda(s, \rho) \left[\left(\frac{d^2 W}{d\rho^2} + \frac{\nu}{\rho} \frac{dW}{d\rho} \right) - I_c^2 \left(\frac{d^4 W}{d\rho^4} + \frac{1}{\rho} \frac{d^3 W}{d\rho^3} - \frac{2}{\rho^2} \frac{d^2 W}{d\rho^2} + \frac{2}{\rho^3} \frac{dW}{d\rho} \right) \right] d\rho \right\} \\ & \quad - \frac{1}{s} \frac{d}{ds} \left\{ \bar{B} \int_0^1 \varphi_\lambda(s, \rho) \left[\left(\nu \frac{dU}{d\rho} + \frac{1}{\rho} U \right) - I_c^2 \left(\frac{1}{\rho} \frac{d^2 U}{d\rho^2} + \frac{1}{\rho^2} \frac{dU}{d\rho} - \frac{1}{\rho^3} U \right) \right] d\rho \right. \\ & \quad \left. - \bar{D} \int_0^1 \varphi_\lambda(s, \rho) \left[\left(\frac{d^2 W}{d\rho^2} + \frac{\nu}{\rho} \frac{dW}{d\rho} \right) - I_c^2 \left(\frac{1}{\rho} \frac{d^3 W}{d\rho^3} + \frac{1}{\rho^2} \frac{d^2 W}{d\rho^2} - \frac{1}{\rho^3} \frac{dW}{d\rho} \right) \right] d\rho \right\} \\ & \quad = \left(\bar{I}_2 \frac{1}{s} \frac{d}{ds} \left(s \frac{dW}{ds} \right) + \bar{I}_1 \frac{1}{s} \frac{d}{ds} (sU) - \bar{I}_0 W \right) \Omega_n^2 \end{aligned} \tag{32-2}$$

Considering eq. (32-2), the high-order BCs, eq. (20) and (31-1), are defined as follows:

$$\begin{cases} I_c^2 \int_0^1 \varphi_\lambda(s, \rho) \left(A \frac{d^2 U}{d\rho^2} - B \frac{d^3 W}{d\rho^3} \right) d\rho = 0 \\ I_c^2 \int_0^1 \varphi_\lambda(s, \rho) \left(B \frac{d^2 U}{d\rho^2} - D \frac{d^3 W}{d\rho^3} \right) d\rho = 0 \end{cases} \quad @ s = 0 \tag{33-1}$$

$$\begin{cases} \bar{A} I_c^2 \int_0^1 \varphi_\lambda(s, \rho) \left(\frac{d^2 u}{d\rho^2} + \nu \left(\frac{1}{r\rho} \frac{du}{d\rho} - \frac{1}{\rho^2} u \right) \right) d\rho \\ \quad - \bar{B} I_c^2 \int_0^1 \varphi_\lambda(s, \rho) \left(\frac{d^3 w}{d\rho^3} + \nu \left(\frac{1}{\rho} \frac{d^2 w}{d\rho^2} - \frac{1}{\rho^2} \frac{dw}{d\rho} \right) \right) d\rho = 0 \\ \bar{B} I_c^2 \int_0^1 \varphi_\lambda(s, \rho) \left(\frac{d^2 u}{d\rho^2} + \nu \left(\frac{1}{r\rho} \frac{du}{d\rho} - \frac{1}{\rho^2} u \right) \right) d\rho \\ \quad - \bar{D} I_c^2 \int_0^1 \varphi_\lambda(s, \rho) \left(\frac{d^3 w}{d\rho^3} + \nu \left(\frac{1}{\rho} \frac{d^2 w}{d\rho^2} - \frac{1}{\rho^2} \frac{dw}{d\rho} \right) \right) d\rho = 0 \end{cases} \quad @ s = 1. \tag{33-2}$$

Similarly, for the BCs introduced in Table 2, the dimensionless BCs are defined as in Table 4.

6. Solution procedure of the governing equations of motion

To solve the governing equations of motion for the circular nano-plate based on the SG model, eqs. (37-1) and (37-2) along with the high-order B. Cs, eqs. (39-1) and (39-2), as well as the introduced B. Cs in Table 3, are used in conjunction with the GDQR method. This method is appropriate for solving sixth-order differential equations with three B. Cs considered individually at its boundary. As will be explained in the sequel, the solution to the governing equations are obtained based on the SG and NSG models.

6.1. Governing equations based on the SG model

According to the GDQR method, the nth-order derivatives of $U(s)$ and $W(s)$ functions at the specified point $s=s_i$ are defined as [59]:

$$\begin{aligned} U^{(n)}(s_i) &= \sum_{k=0}^1 g_{1k}^{(n)}(s_i) U_1^{(k)} + \sum_{j=2}^{N-1} g_{j0}^{(n)}(s_i) U_j^{(k)} + \sum_{k=0}^1 g_{Nk}^{(n)}(s_i) U_N^{(k)} = \sum_{k=1}^{N+2} E_{ik}^{(n)} \Psi_k \\ W^{(n)}(s_i) &= \sum_{k=0}^2 h_{1k}^{(n)}(s_i) W_1^{(k)} + \sum_{j=2}^{N-1} h_{j0}^{(n)}(s_i) W_j^{(k)} + \sum_{k=0}^2 h_{Nk}^{(n)}(s_i) W_N^{(k)} = \sum_{k=1}^{N+4} F_{ik}^{(n)} \Theta_k \end{aligned} \tag{34}$$

where

$$\begin{aligned} \{E_{ik}^{(n)}\}^T &= \{g_{10}^{(n)}(r_i), g_{11}^{(n)}(r_i), g_{20}^{(n)}(r_i), \dots, g_{(N-1)0}^{(n)}(r_i), g_{N0}^{(n)}(r_i), g_{N1}^{(n)}(r_i)\} \\ \{F_{ik}^{(n)}\}^T &= \{h_{10}^{(n)}(r_i), h_{11}^{(n)}(r_i), h_{12}^{(n)}(r_i), h_{20}^{(n)}(r_i), \dots, h_{(N-1)0}^{(n)}(r_i), h_{N0}^{(n)}(r_i), h_{N1}^{(n)}(r_i), h_{N2}^{(n)}(r_i)\} \end{aligned} \tag{35-1}$$



Table 4. Dimensionless BCs based on NSG model in frequency space.

Boundary type	Boundary condition
Center of plate	$U = \frac{dW}{ds} = 0$ $Q_r = 0 \Rightarrow \int_0^1 \varphi_\lambda(s, \rho) \left\{ \bar{B} \left(\frac{d^2U}{d\rho^2} - L_c^2 \frac{d^4U}{d\rho^4} \right) - \bar{D} \left(\frac{d^3W}{d\rho^3} - L_c^2 \frac{d^5W}{d\rho^5} \right) \right\} d\rho = 0.$
Clamped	$U = W = \frac{dW}{ds} = 0$
Simply supported	$U = W = 0,$ $M_r = 0 \Rightarrow \bar{B} \int_0^1 \varphi_\lambda(s, \rho) \left\{ \left(\frac{dU}{d\rho} + \frac{\nu}{\rho} U \right) - L_c^2 \left(\frac{d^3U}{d\rho^3} + \frac{1}{\rho} \frac{d^2U}{d\rho^2} - \frac{2}{\rho^2} \frac{dU}{d\rho} + \frac{2}{\rho^3} U \right) \right\} d\rho$ $- \bar{D} \int_0^1 \varphi_\lambda(s, \rho) \left\{ \left(\frac{d^2W}{d\rho^2} + \frac{\nu}{\rho} \frac{dW}{d\rho} \right) - L_c^2 \left(\frac{d^4W}{d\rho^4} + \frac{1}{\rho} \frac{d^3W}{d\rho^3} - \frac{2}{\rho^2} \frac{d^2W}{d\rho^2} + \frac{2}{\rho^3} \frac{dW}{d\rho} \right) \right\} d\rho = 0.$
Free	$N_r = 0 \Rightarrow \bar{A} \int_0^1 \varphi_\lambda(s, \rho) \left\{ \left(\frac{dU}{d\rho} + \frac{\nu}{\rho} U \right) - L_c^2 \left(\frac{d^3U}{d\rho^3} + \frac{1}{\rho} \frac{d^2U}{d\rho^2} - \frac{2}{\rho^2} \frac{dU}{d\rho} + \frac{2}{\rho^3} U \right) \right\} d\rho$ $- \bar{B} \int_0^1 \varphi_\lambda(s, \rho) \left\{ \left(\frac{d^2W}{d\rho^2} + \frac{\nu}{\rho} \frac{dW}{d\rho} \right) - L_c^2 \left(\frac{d^4W}{d\rho^4} + \frac{1}{\rho} \frac{d^3W}{d\rho^3} - \frac{2}{\rho^2} \frac{d^2W}{d\rho^2} + \frac{2}{\rho^3} \frac{dW}{d\rho} \right) \right\} d\rho = 0,$ $Q_r = 0 \Rightarrow \int_0^1 \varphi_\lambda(s, \rho) \left\{ \bar{B} \left(\frac{d^2U}{d\rho^2} + \frac{1}{\rho} \frac{dU}{d\rho} - \frac{1}{\rho^2} U \right) - \bar{D} \left(\frac{d^3W}{d\rho^3} + \frac{1}{\rho} \frac{d^2W}{d\rho^2} - \frac{1}{\rho^2} \frac{dW}{d\rho} \right) \right\} d\rho$ $- \bar{B} L_c^2 \int_0^1 \varphi_\lambda(s, \rho) \left(\frac{d^4U}{d\rho^4} + \frac{2}{\rho} \frac{\partial^3U}{\partial \rho^3} - \frac{3}{\rho^2} \frac{\partial^2U}{\partial \rho^2} + \frac{3}{\rho^3} \frac{\partial U}{\partial \rho} - \frac{3}{\rho^4} U \right) d\rho$ $+ \bar{D} L_c^2 \int_0^1 \varphi_\lambda(s, \rho) \left(\frac{d^5W}{d\rho^5} + \frac{2}{\rho} \frac{d^4W}{d\rho^4} - \frac{3}{\rho^2} \frac{d^3W}{d\rho^3} + \frac{3}{\rho^3} \frac{d^2W}{d\rho^2} - \frac{3}{\rho^4} \frac{\partial W}{\partial \rho} \right) d\rho = 0,$ $M_r = 0 \Rightarrow \bar{B} \int_0^1 \varphi_\lambda(s, \rho) \left\{ \left(\frac{dU}{d\rho} + \frac{\nu}{\rho} U \right) - L_c^2 \left(\frac{d^3U}{d\rho^3} + \frac{1}{\rho} \frac{d^2U}{d\rho^2} - \frac{2}{\rho^2} \frac{dU}{d\rho} + \frac{2}{\rho^3} U \right) \right\} d\rho$ $- \bar{D} \int_0^1 \varphi_\lambda(s, \rho) \left\{ \left(\frac{d^2W}{d\rho^2} + \frac{\nu}{\rho} \frac{dW}{d\rho} \right) - L_c^2 \left(\frac{d^4W}{d\rho^4} + \frac{1}{\rho} \frac{d^3W}{d\rho^3} - \frac{2}{\rho^2} \frac{d^2W}{d\rho^2} + \frac{2}{\rho^3} \frac{dW}{d\rho} \right) \right\} d\rho = 0.$

$$\begin{aligned} \{\Psi_1, \Psi_2, \dots, \Psi_j, \dots, \Psi_{N+2}\} &= \{U_1, U_1^{(1)}, U_2, \dots, U_N, U_N^{(1)}\} \\ \{\Theta_1, \Theta_2, \dots, \Theta_j, \dots, \Theta_{N+4}\} &= \{W_1, W_1^{(1)}, W_1^{(2)}, W_2, \dots, W_N, W_N^{(1)}, W_N^{(2)}\} \end{aligned} \tag{35-2}$$

$$s_i = \frac{1}{2} \left(1 - \cos \left(\frac{i-1}{N-1} \pi \right) \right) \tag{35-3}$$

In the above equations, N represents the total number of discrete grid points along r direction. The weighting coefficients in eq. (34) are defined as follows:

$$\begin{cases} g_{ki}(x) = (a_{ki}x^2 + b_{ki}x + c_{ki})L_1(x) & (i = 0, 1), (k = 1, N) \\ g_{j0}(x) = \frac{(x - x_1)(x - x_N)}{(x_j - x_1)(x_j - x_N)}L_j(x) & (j = 2, 3, \dots, N - 1) \end{cases} \tag{36-1}$$

$$\begin{cases} h_{ki}(x) = \frac{(x - x_N)^2}{(x_1 - x_N)^2} (\bar{a}_{ki}x^2 + \bar{b}_{ki}x + \bar{c}_{ki})L_1(x) & (i = 0, 1, 2), (k = 1, N) \\ h_{j0}(x) = \frac{(x - x_1)^2(x - x_N)^2}{(x_j - x_1)^2(x_j - x_N)^2}L_j(x) & (j = 2, 3, \dots, N - 1) \end{cases} \tag{36-2}$$

where

$$\begin{cases} a_{10} = \frac{-1}{(x_1 - x_N)^2} - \frac{L_1^{(1)}(x_1)}{(x_1 - x_N)}, & b_{10} = \frac{1}{(x_1 - x_N)} - a_{10}(x_1 + x_N), & c_{10} = 1 - a_{10}x_1^2 - b_{10}x_1, \\ a_{11} = \frac{1}{(x_1 - x_N)}, & b_{10} = -\frac{(x_1 + x_N)}{(x_1 - x_N)}, & c_{10} = \frac{x_1x_N}{(x_1 - x_N)}, \end{cases} \tag{37-1}$$



$$\begin{cases} a_{N0} = \frac{-1}{(x_1 - x_N)^2} + \frac{L_1^{(N)}(x_N)}{(x_1 - x_N)}, & b_{N0} = \frac{-1}{(x_1 - x_N)} - a_{N0}(x_1 + x_N), & c_{N0} = 1 - a_{N0}x_N^2 - b_{N0}x_N, \\ a_{N1} = \frac{-1}{(x_1 - x_N)}, & b_{N0} = \frac{(x_1 + x_N)}{(x_1 - x_N)}, & c_{N0} = \frac{-x_1x_N}{(x_1 - x_N)}. \end{cases} \tag{37-2}$$

$$\begin{cases} \bar{a}_{10} = \left(L_1^{(1)}(x_1) + \frac{2}{x_1 - x_N} \right)^2 - \frac{L_1^{(2)}(x_1)}{2} - \frac{1}{(x_1 - x_N)^2} - \frac{2L_1^{(1)}(x_1)}{x_1 - x_N} \\ \bar{b}_{10} = - \left(L_1^{(1)}(x_1) + \frac{2}{x_1 - x_N} \right) - 2\bar{a}_{10}x_1, & c_{10} = 1 + \bar{a}_{10}x_1^2 + x_1 \left(L_1^{(1)}(x_1) + \frac{2}{x_1 - x_N} \right) \\ \bar{a}_{11} = - \left(L_1^{(1)}(x_1) + \frac{2}{x_1 - x_N} \right)^2, & \bar{b}_{11} = 1 - 2\bar{a}_{10}x_1, & \bar{c}_{11} = x_1(\bar{a}_{11}x_1 - 1), & \bar{a}_{12} = \frac{1}{2}, & \bar{b}_{12} = -x_1, & \bar{c}_{12} = \frac{x_1^2}{2}. \end{cases} \tag{37-3}$$

$$\begin{cases} \bar{a}_{N0} = \left(L_N^{(1)}(x_N) - \frac{2}{x_1 - x_N} \right)^2 - \frac{L_N^{(2)}(x_N)}{2} - \frac{1}{(x_1 - x_N)^2} + \frac{2L_N^{(1)}(x_N)}{x_1 - x_N}, \\ \bar{b}_{N0} = - \left(L_N^{(1)}(x_N) - \frac{2}{x_1 - x_N} \right) - 2\bar{a}_{N0}x_N, & c_{N0} = 1 + \bar{a}_{N0}x_N^2 + x_N \left(L_N^{(1)}(x_N) - \frac{2}{x_1 - x_N} \right), \\ \bar{a}_{N1} = - \left(L_N^{(1)}(x_N) - \frac{2}{x_1 - x_N} \right)^2, & \bar{b}_{N1} = 1 - 2\bar{a}_{N0}x_N, & \bar{c}_{N1} = x_N(\bar{a}_{N1}x_N - 1), \\ \bar{a}_{N2} = \frac{1}{2}, & \bar{b}_{N2} = -x_N, & \bar{c}_{N2} = \frac{x_N^2}{2}. \end{cases} \tag{37-4}$$

In the above relations, $L(x)$ denotes the Legendre interpolation function with the following properties [59]:

$$L_i(x_j) = \begin{cases} 1 & i=j \\ 0 & i \neq j \end{cases} \tag{38}$$

The first and second derivatives of $L(x)$ are also available in references [60, 61]. Now, using eq. (34), the equations of motion represented in (27-1) and (27-2) can be rewritten as:

$$\begin{aligned} \bar{A} \left(\sum_{k=1}^{N+4} E_{ik}^{(2)} \Psi_k + \frac{1}{s} \sum_{k=1}^{N+4} E_{ik}^{(1)} \Psi_k - \frac{1}{s^2} U_i \right) - L_c^2 \left(\sum_{k=1}^{N+4} F_{ik}^{(4)} \Psi_k - \frac{\nu - 1}{s} \sum_{k=1}^{N+4} F_{ik}^{(3)} \Psi_k \right) \\ - \bar{B} \left(\sum_{k=1}^{N+4} F_{ik}^{(3)} \Theta_k + \frac{1}{s} \sum_{k=1}^{N+4} F_{ik}^{(2)} \Theta_k - \frac{1}{s^2} \sum_{k=1}^{N+4} F_{ik}^{(1)} \Theta_k \right) - L_c^2 \left(\sum_{k=1}^{N+4} F_{ik}^{(5)} \Theta_k - \frac{\nu - 1}{s} \sum_{k=1}^{N+4} F_{ik}^{(4)} \Theta_k \right) \\ = \left(\bar{I}_1 \sum_{k=1}^{N+4} F_{ik}^{(1)} \Theta_k - \bar{I}_2 U_i \right) \Omega_n^2 \end{aligned} \tag{39-1}$$

$$\begin{aligned} \bar{B} \left(\sum_{k=1}^{N+4} F_{ik}^{(3)} \Psi_k + \frac{2}{s} \sum_{k=1}^{N+4} F_{ik}^{(2)} \Psi_k - \frac{1}{s^2} \sum_{k=1}^{N+4} E_{ik}^{(1)} \Psi_k + \frac{1}{s^3} U \right) - L_c^2 \left(\sum_{k=1}^{N+4} E_{ik}^{(5)} \Psi_k - \frac{\nu - 2}{s} \sum_{k=1}^{N+4} F_{ik}^{(4)} \Psi_k \right) \\ - \bar{D} \left(\sum_{k=1}^{N+4} F_{ik}^{(4)} \Theta_k + \frac{2}{s} \sum_{k=1}^{N+4} F_{ik}^{(3)} \Theta_k - \frac{1}{s^2} \sum_{k=1}^{N+4} F_{ik}^{(2)} \Theta_k + \frac{1}{s^3} \sum_{k=1}^{N+4} F_{ik}^{(1)} \Theta_k \right) - L_c^2 \left(\sum_{k=1}^{N+4} F_{ik}^{(6)} \Theta_k - \frac{\nu - 2}{s} \sum_{k=1}^{N+4} F_{ik}^{(5)} \Theta_k \right) \\ = \left(\bar{I}_2 \left(\sum_{k=1}^{N+4} F_{ik}^{(2)} \Theta_k + \frac{1}{s} \sum_{k=1}^{N+4} F_{ik}^{(1)} \Theta_k \right) - \bar{I}_1 \left(\sum_{k=1}^{N+4} E_{ik}^{(1)} \Psi_k + \frac{1}{s} U \right) - \bar{I}_3 W_i \right) \Omega_n^2 \end{aligned} \tag{39-2}$$

Additionally, the high-order BCs are expressed as follows:

$$L_c^2 \left(\bar{A} \sum_{k=1}^{N+4} E_{1k}^{(2)} \Psi_k - \bar{B} \sum_{k=1}^{N+4} F_{1k}^{(3)} \Theta_k \right) = 0, \quad L_c^2 \left(\bar{B} \sum_{k=1}^{N+4} E_{1k}^{(2)} \Psi_k - \bar{D} \sum_{k=1}^{N+4} F_{1k}^{(3)} \Theta_k \right) = 0. \tag{40-1}$$

$$\begin{aligned} \bar{A} L_c^2 \left(\sum_{k=1}^{N+4} E_{Nk}^{(2)} \Psi_k + \nu \left(\sum_{k=1}^{N+4} E_{Nk}^{(1)} \Psi_k - U_N \right) \right) - \bar{B} L_c^2 \left(\sum_{k=1}^{N+4} F_{Nk}^{(3)} \Theta_k + \nu \left(\sum_{k=1}^{N+4} F_{Nk}^{(3)} \Theta_k - \sum_{k=1}^{N+4} F_{Nk}^{(1)} \Theta_k \right) \right) = 0, \\ \bar{B} L_c^2 \left(\sum_{k=1}^{N+4} E_{Nk}^{(2)} \Psi_k + \nu \left(\sum_{k=1}^{N+4} E_{Nk}^{(1)} \Psi_k - U_N \right) \right) - \bar{D} L_c^2 \left(\sum_{k=1}^{N+4} F_{Nk}^{(3)} \Theta_k + \nu \left(\sum_{k=1}^{N+4} F_{Nk}^{(3)} \Theta_k - \sum_{k=1}^{N+4} F_{Nk}^{(1)} \Theta_k \right) \right) = 0. \end{aligned} \tag{40-2}$$

The BCs at the nano-plate center are defined as:

$$U_1 = 0, \quad \sum_{k=1}^{N+4} F_{1k}^{(1)} \Theta_k = 0, \quad \bar{B} \left(\sum_{k=1}^{N+4} E_{1k}^{(1)} \Psi_k \right) - \bar{D} \left(\sum_{k=1}^{N+4} F_{1k}^{(1)} \Theta_k \right) = 0. \tag{41}$$

Moreover, the corresponding BCs for the cases of clamped, simply-supported, and free-edge are defined as:

$$U_N = U_N = \sum_{k=1}^{N+4} F_{Nk}^{(1)} \Theta_k = 0. \tag{42-1}$$



$$\begin{cases} U_N = W_N = 0 \\ M_{rr} = \bar{B} \left(\sum_{k=1}^{N+4} E_{Nk}^{(1)} \Psi_k + \frac{\nu}{s} U_N - L_c^2 \sum_{k=1}^{N+4} E_{Nk}^{(3)} \Psi_k \right) - D \left(\sum_{k=1}^{N+4} F_{Nk}^{(2)} \Theta_k + \frac{\nu}{s} \sum_{k=1}^{N+4} F_{Nk}^{(1)} \Theta_k - L_c^2 \sum_{k=1}^{N+4} F_{Nk}^{(4)} \Theta_k \right) = 0 \end{cases} \quad (42-2)$$

$$\begin{cases} N_{rr} = \bar{A} \left(\sum_{k=1}^{N+4} E_{Nk}^{(1)} \Psi_k + \nu U_N - L_c^2 \sum_{k=1}^{N+4} E_{Nk}^{(3)} \Psi_k \right) - \bar{B} \left(\sum_{k=1}^{N+4} F_{Nk}^{(2)} \Theta_k + \nu \sum_{k=1}^{N+4} F_{Nk}^{(1)} \Theta_k - L_c^2 \sum_{k=1}^{N+4} F_{Nk}^{(4)} \Theta_k \right) = 0 \\ Q_r = \bar{B} \left(\sum_{k=1}^{N+4} E_{Nk}^{(2)} \Psi_k + \sum_{k=1}^{N+4} E_{Nk}^{(1)} \Psi_k - U_N - L_c^2 \left(\sum_{k=1}^{N+4} E_{Nk}^{(4)} \Psi_k - (\nu - 1) \sum_{k=1}^{N+4} E_{Nk}^{(3)} \Psi_k \right) \right) \\ \quad - \bar{D} \left(\sum_{k=1}^{N+4} F_{Nk}^{(3)} \Theta_k + \sum_{k=1}^{N+4} F_{Nk}^{(2)} \Theta_k - \sum_{k=1}^{N+4} F_{Nk}^{(1)} \Theta_k - L_c^2 \left(\sum_{k=1}^{N+4} F_{Nk}^{(5)} \Theta_k - (\nu - 1) \sum_{k=1}^{N+4} F_{Nk}^{(4)} \Theta_k \right) \right) = 0 \\ M_{rr} = \bar{B} \left(\sum_{k=1}^{N+4} E_{Nk}^{(1)} \Psi_k + \nu U_N - L_c^2 \sum_{k=1}^{N+4} E_{Nk}^{(3)} \Psi_k \right) - \bar{D} \left(\sum_{k=1}^{N+4} F_{Nk}^{(2)} \Theta_k + \nu \sum_{k=1}^{N+4} F_{Nk}^{(1)} \Theta_k - L_c^2 \sum_{k=1}^{N+4} F_{Nk}^{(4)} \Theta_k \right) = 0 \end{cases} \quad (42-3)$$

These algebraic equations can be rearranged as follows:

$$\begin{bmatrix} [S_{bb}] & [S_{bd}] \\ [S_{db}] & [S_{dd}] \end{bmatrix} \begin{Bmatrix} \{U_b\} \\ \{U_d\} \end{Bmatrix} - \Omega_n^2 \begin{bmatrix} [0] & [0] \\ [Q_{db}] & [Q_{dd}] \end{bmatrix} \begin{Bmatrix} \{U_b\} \\ \{U_d\} \end{Bmatrix} = \begin{Bmatrix} \{0\} \\ \{0\} \end{Bmatrix} \quad (43)$$

where

$$\begin{aligned} \{U_b\} &= \{U_1, U_2, U_3, U_4, U_5, U_{2N+2}, U_{2N+3}, U_{2N+4}, U_{2N+5}, U_{2N+6}\} \\ &= \{W_1^{(2)}, U_1^{(1)}, W_1^{(1)}, U_1, W_1, U_N, W_N, U_N^{(1)}, W_N^{(1)}, W_N^{(2)}\} \end{aligned} \quad (44-1)$$

$$\{U_d\} = \{U_6, U_7, \dots, U_{2N}, U_{2N+1}\} = \{U_2, W_2, U_3, W_3, \dots, U_{N-2}, W_{N-2}, U_{N-1}, W_{N-1}\} \quad (44-2)$$

Rewriting eqs. (44-1) and (44-2) in a simple form, we have:

$$([S] - \Omega_n^2 [Q]) \{U_d\} = \{0\} \quad (45)$$

where

$$[S] = [S_{dd}] - [S_{db}] [S_{bb}]^{-1} [S_{bd}] \quad , \quad [Q] = [Q_{dd}] - [Q_{db}] [S_{bb}]^{-1} [S_{bd}] \quad (46)$$

Solving the eigenvalue equation obtained as eq. (45), the dimensionless frequencies Ω_n and the corresponding mode shapes, $\{U_b\}$ and $\{U_d\}$ can be obtained.

6.2. Solution of governing equations based on the NSG model

To solve the governing equations of the nano-plate based on the NSG model, the Galerkin weighted residual method is used. According to this method, the solution to eqs. (32-1) and (32-2) is assumed to be;

$$\{U(s), W(s)\} = \sum_{j=1}^{Nm} \{a_j U_j(s), b_j W_j(s)\} \quad (47)$$

where a_j and b_j are the unknown coefficients, and $U_j(s)$ and $W_j(s)$ are the mode shapes of the circular nano-plate resulting from the GDQR numerical solution based on the SG model. Also, N_m is the number of modes used in the Galerkin method. For this purpose, it is required that eq. (47) satisfies all natural and geometric classical boundary conditions in Table 4, as well as the higher-order BCs given in eqs. (33-1) and (33-2).

Substituting eq. (47) in eqs. (32-1) and (32-2), one can express the residual functions as:

$$\begin{aligned} R_1(a_j, \omega_n) &= \frac{1}{s} \frac{d}{ds} \left[\bar{A} s \int_0^1 \varphi_\lambda(s, \rho) \sum_{j=1}^{Nm} a_j \left\{ \left(\frac{dU_j}{d\rho} + \frac{\nu}{\rho} U_j \right) - L_c^2 \left(\frac{d^3 U_j}{d\rho^3} + \frac{1}{\rho} \frac{d^2 U_j}{d\rho^2} - \frac{2}{\rho^2} \frac{dU_j}{d\rho} + \frac{2}{\rho^3} U_j \right) \right\} d\rho \right. \\ &\quad \left. - \bar{B} s \int_0^1 \varphi_\lambda(s, \rho) \sum_{j=1}^{Nm} b_j \left\{ \left(\frac{d^2 W_j}{d\rho^2} + \frac{\nu}{\rho} \frac{\partial W_j}{\partial \rho} \right) - L_c^2 \left(\frac{d^4 W}{d\rho^4} + \frac{1}{\rho} \frac{d^3 W_j}{d\rho^3} - \frac{2}{\rho^2} \frac{d^2 W_j}{d\rho^2} + \frac{2}{\rho^3} \frac{dW_j}{d\rho} \right) \right\} d\rho \right] \\ &\quad - \frac{1}{s} \left[\bar{A} \int_0^1 \varphi_\lambda(s, \rho) \sum_{j=1}^{Nm} a_j \left\{ \left(\nu \frac{dU_j}{d\rho} + \frac{1}{\rho} U_j \right) - L_c^2 \left(\frac{1}{\rho} \frac{d^2 U_j}{d\rho^2} + \frac{1}{\rho^2} \frac{dU_j}{d\rho} - \frac{1}{\rho^3} U_j \right) \right\} d\rho \right. \\ &\quad \left. - \frac{1}{s} \bar{B} \int_0^1 \varphi_\lambda(s, \rho) \sum_{j=1}^{Nm} b_j \left\{ \left(\frac{d^2 W_j}{d\rho^2} + \frac{\nu}{\rho} \frac{dW_j}{d\rho} \right) - L_c^2 \left(\frac{1}{\rho} \frac{d^3 W_j}{d\rho^3} + \frac{1}{\rho^2} \frac{d^2 W_j}{d\rho^2} - \frac{1}{\rho^3} \frac{dW_j}{d\rho} \right) \right\} d\rho \right] \\ &\quad - \left(I_1 \sum_{j=1}^{Nm} b_j \frac{dW_j}{ds} - I_0 \sum_{j=1}^{Nm} a_j U_j(s) \right) \Omega_n^2 \end{aligned} \quad (48-1)$$



$$\begin{aligned}
 R_2(a_j, \omega_n) = & \bar{B} \int_0^1 \varphi_\lambda(s, \rho) \sum_{j=1}^{Nm} a_j \left\{ \begin{aligned} & \frac{d^3 U_j}{d\rho^3} + \frac{2}{\rho} \frac{d^2 U_j}{d\rho^2} - \frac{1}{\rho^2} \frac{dU_j}{d\rho} + \frac{1}{\rho^3} U_j \\ & - I_c^2 \left(\frac{d^5 U_j}{d\rho^5} + \frac{3}{\rho} \frac{d^4 U_j}{d\rho^4} - \frac{3}{\rho^2} \frac{d^3 U_j}{d\rho^3} + \frac{6}{\rho^3} \frac{d^2 U_j}{d\rho^2} - \frac{9}{\rho^4} \frac{dU_j}{d\rho} + \frac{9}{\rho^5} U_j \right) \end{aligned} \right\} d\rho \\
 & + \bar{D} \int_0^1 \varphi_\lambda(s, \rho) \sum_{j=1}^{Nm} b_j \left\{ \begin{aligned} & \frac{d^4 W_j}{d\rho^4} + \frac{2}{\rho} \frac{d^3 W_j}{d\rho^3} - \frac{1}{\rho^2} \frac{d^2 W_j}{d\rho^2} + \frac{1}{\rho^3} \frac{dW_j}{d\rho} \\ & - I_c^2 \left(\frac{d^6 W_j}{d\rho^6} + \frac{3}{\rho} \frac{d^5 W_j}{d\rho^5} - \frac{3}{\rho^2} \frac{d^4 W_j}{d\rho^4} + \frac{6}{\rho^3} \frac{d^3 W_j}{d\rho^3} - \frac{9}{\rho^4} \frac{d^2 W_j}{d\rho^2} + \frac{9}{\rho^5} \frac{dW_j}{d\rho} \right) \end{aligned} \right\} d\rho \\
 & - \left[\bar{I}_2 \left(\frac{1}{s} \frac{d}{ds} \left(s \sum_{j=1}^{Nm} b_j \frac{dW_j}{ds} \right) \right) + \bar{I}_1 \left(\frac{1}{s} \frac{d}{ds} \left(s \sum_{j=1}^{Nm} a_j U_j(s) \right) \right) - \bar{I}_0 \sum_{j=1}^{Nm} b_j W_j \right] \Omega_n^2
 \end{aligned} \tag{48-2}$$

Using the Galerkin method for the residual functions will result in eq. (49) such that;

$$\sum_{j=1}^{Nm} \{ k_{ij}^{11} a_j + k_{ij}^{12} b_j - (m_{ij}^{11} a_j + m_{ij}^{12} b_j) \Omega_n^2 \} = 0 \quad , \quad \sum_{j=1}^{Nm} \{ k_{ij}^{21} a_j + k_{ij}^{22} b_j - (m_{ij}^{21} a_j + m_{ij}^{22} b_j) \Omega_n^2 \} = 0. \tag{49}$$

where

$$\begin{aligned}
 m_{ij}^{11} = & -I_0 \int_0^1 U_i U_j ds \quad , \quad m_{ij}^{12} = I_1 \int_0^1 U_i \frac{dW_j}{ds} ds, \\
 m_{ij}^{21} = & \int_0^1 \left\{ \bar{I}_2 W_i \left(\frac{1}{s} \frac{d}{ds} \left(s \frac{dW_j}{ds} \right) \right) - \bar{I}_0 W_i W_j \right\} ds, \quad m_{ij}^{22} = \bar{I} \int_0^1 \left\{ {}_1 W_i \left(\frac{1}{s} \frac{d}{ds} (s U_j) \right) \right\} ds.
 \end{aligned} \tag{50-1}$$

$$\begin{aligned}
 k_{ij}^{11} = & \bar{A} \int_0^1 U_i \int_0^1 \varphi_\lambda(s, \rho) \left\{ \left(\frac{d^2 U_j}{d\rho^2} + \frac{1}{\rho} \frac{\partial U_j}{\partial \rho} - \frac{1}{\rho^2} U_j \right) \right. \\
 & \left. - I_c^2 \left(\frac{d^4 U_j}{d\rho^4} + \frac{2}{\rho} \frac{d^3 U_j}{d\rho^3} - \frac{3}{\rho^2} \frac{d^2 U_j}{d\rho^2} + \frac{3}{\rho^3} \frac{dU_j}{d\rho} - \frac{3}{\rho^4} U_j \right) \right\} d\rho ds, \\
 k_{ij}^{12} = & \bar{B} \int_0^1 U_i \int_0^1 \varphi_\lambda(s, \rho) \left\{ \left(\frac{d^3 W_j}{d\rho^3} + \frac{1}{\rho} \frac{d^2 W_j}{d\rho^2} - \frac{1}{\rho^2} \frac{dW_j}{d\rho} \right) \right. \\
 & \left. - I_c^2 \left(\frac{d^5 W_j}{d\rho^5} + \frac{2}{\rho} \frac{d^4 W_j}{d\rho^4} - \frac{3}{\rho^2} \frac{d^3 W_j}{d\rho^3} + \frac{3}{\rho^3} \frac{d^2 W_j}{d\rho^2} - \frac{3}{\rho^4} \frac{dW_j}{d\rho} \right) \right\} d\rho ds,
 \end{aligned} \tag{50-2}$$

$$\begin{aligned}
 k_{ij}^{21} = & \bar{B} \int_0^1 U_i \int_0^1 \varphi_\lambda(s, \rho) \left\{ \left(\frac{d^3 U_j}{d\rho^3} + \frac{2}{\rho} \frac{d^2 U_j}{d\rho^2} - \frac{1}{\rho^2} \frac{dU_j}{d\rho} + \frac{1}{\rho^3} U_j \right) \right. \\
 & \left. - I_c^2 \left(\frac{d^5 U_j}{d\rho^5} + \frac{3}{\rho} \frac{d^4 U_j}{d\rho^4} - \frac{3}{\rho^2} \frac{d^3 U_j}{d\rho^3} + \frac{6}{\rho^3} \frac{d^2 U_j}{d\rho^2} - \frac{9}{\rho^4} \frac{dU_j}{d\rho} + \frac{9}{\rho^5} U_j \right) \right\} d\rho ds, \\
 k_{ij}^{22} = & \bar{D} \int_0^1 U_i \int_0^1 \varphi_\lambda(s, \rho) \left\{ \left(\frac{d^4 W_j}{d\rho^4} + \frac{2}{\rho} \frac{d^3 W_j}{d\rho^3} - \frac{1}{\rho^2} \frac{d^2 W_j}{d\rho^2} + \frac{1}{\rho^3} \frac{dW_j}{d\rho} \right) \right. \\
 & \left. - I_c^2 \left(\frac{d^6 W_j}{d\rho^6} + \frac{3}{\rho} \frac{d^5 W_j}{d\rho^5} - \frac{3}{\rho^2} \frac{d^4 W_j}{d\rho^4} + \frac{6}{\rho^3} \frac{d^3 W_j}{d\rho^3} - \frac{9}{\rho^4} \frac{d^2 W_j}{d\rho^2} + \frac{9}{\rho^5} \frac{dW_j}{d\rho} \right) \right\} d\rho ds
 \end{aligned} \tag{50-3}$$

Equation (59) can be recast in the simple form of:

$$([K] - \Omega_n^2 [M]) \{q\} = \{0\} \tag{51}$$

where

$$[K] = \begin{bmatrix} k_{ij}^{11} & k_{ij}^{12} \\ k_{ij}^{21} & k_{ij}^{22} \end{bmatrix} \quad , \quad [M] = \begin{bmatrix} m_{ij}^{11} & m_{ij}^{12} \\ m_{ij}^{21} & m_{ij}^{22} \end{bmatrix} \quad , \quad \{q\} = \begin{bmatrix} a_j \\ b_j \end{bmatrix} \tag{52}$$

Solving the eigenvalue problem of eq. (51), the dimensionless frequencies Ω_n and the corresponding mode shapes $\{q\}$ can be determined.

7. Validation of the solution procedure

Since there are no published results in the literature for the vibrational analysis of the FGM circular nano-plate based on the integral form of the NSGT, then, the results in Ref. [62] based on the SGT, as well as the nonlocal elasticity (in Ref. [11]) are used as a comparison/validation of the current findings that are based on GDQR method. In Ref. [62], the influence of non-dimensional scale parameter h/L on the first axisymmetric natural frequency was evaluated using the classical plate theory and the SGT based on the simply supported B.C. The properties of the micro-plate in question are given in Table 5.



Table 5. Mechanical properties of the circular micro-plate.

E_c (Gpa)	E_m (Gpa)	ρ_c (Kg/m ³)	ρ_m (Kg/m ³)	ν
427	70	3100	2702	0.33

Table 6. Comparison of the dimensionless natural frequencies obtained from the GDQR method and Ref. [62] for the first mode of axisymmetrical natural frequency under simply supported BCs, with $N=10$.

BCs	Results	$\Omega_1 = R^2 \sqrt{\frac{I_0}{D}} \omega_1$					
		$h/L=0.5$	$h/L=1.0$	$h/L=1.5$	$h/L=2.0$	$h/L=2.5$	$h/L=5.0$
Simply supported	Ref. [62]	8.71	4.33	3.02	2.31	1.95	1.29
	GDQR	8.72	4.33	3.03	2.31	1.96	1.30

Table 7. Comparison of dimensionless natural frequencies obtained from the GDQR method and those in Ref. [11] for the first four modes of vibration under simply supported and clamped BCs, with $N=10$.

BCs	Mode number	Results	$\Omega_n = R^2 \sqrt{\frac{I_0}{D}} \omega_n$				
			$e_0a/R=0$	$e_0a=0.05$	$e_0a=0.10$	$e_0a=0.15$	$e_0a=0.20$
Simply supported	1	Ref. [11]	4.9344	4.8821	4.7799	4.6133	4.4450
		GDQR	4.9455	4.8925	4.7889	4.622	4.4740
	2	Ref. [11]	29.9455	28.8795	26.2564	23.1263	20.1755
		GDQR	29.9544	28.8815	26.2501	23.1303	20.1815
	3	Ref. [11]	74.3712	68.2841	56.3010	23.1263	20.1755
		GDQR	74.3812	68.2911	56.3120	23.1303	20.1835
	4	Ref. [11]	138.5286	119.3771	89.6747	67.2535	51.1461
		GDQR	138.5336	119.3811	89.6837	67.2615	51.1421
Clamped	1	Ref. [11]	10.2138	10.1012	9.8794	9.5566	9.0338
		GDQR	10.2228	10.1122	9.8614	9.5472	9.0288
	2	Ref. [11]	39.7711	38.0047	33.8497	29.1927	25.0443
		GDQR	39.7821	38.0117	33.8537	29.2068	25.0988
	3	Ref. [11]	89.1039	80.7701	65.1939	51.8517	42.1350
		GDQR	89.11079	80.7841	65.2076	51.8608	42.1384
	4	Ref. [11]	158.1836	134.2385	98.9751	74.5920	58.8814
		GDQR	158.1876	134.2402	98.9699	74.5965	58.899

Moreover, using the DGQR method, the first axisymmetrical frequency was calculated for different values of the non-dimensional scale parameters of $h/L=0, 1.0, 1.5, 2.5,$ and $5.0.$ and the resulting values were compared with their counterparts in Ref. [62], as shown in Table 6. In this case, the total number of discrete grid points along r direction in the GDQR method was chosen as $N=10.$ This comparison confirms the accuracy of the proposed procedure in this analysis.

Furthermore, the vibrational behavior of a circular nano-plate was studied in Ref. [11]. In this reference, the influence of non-dimensional scale parameter $e_0a/R,$ on the axisymmetrical natural frequency was evaluated using the classical plate theory and elasticity for simply supported and clamped BCs. The first four axisymmetric frequencies were calculated using the GDQR method for values of the non-dimensional scale parameters, $e_0/R=0, 0.05, 0.10, 0.15,$ and $0.20,$ and compared with their counterpart values in Ref. [11]. This comparison is shown in Table 7. In this case, the total number of discrete grid points along r direction was selected as $N=10.$ This comparison confirms the accuracy of the proposed procedure in this analysis.

Finally, to evaluate the convergence of the results obtained from the GDQR method, the first four dimensional axisymmetric natural frequencies of the circular nano-plate with clamped, simply-supported, and free BCs with $h/R = 0.01, \nu=0.33$ and $n=1,$ as well as three size parameters of $L_c=0.01, 0.05, 0.10$ are shown in Figs. 3 to 6. According to these figures, the convergence occurs at $N=15.$

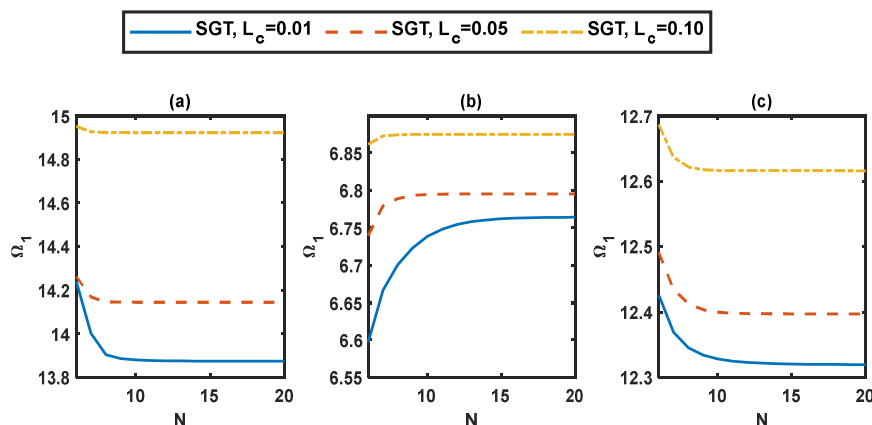


Fig. 3. Evaluating the convergence of the first mode for (a) clamped, (b) simply-supported, and (c) free BCs for $h/R=0.01, \nu=0.33,$ and $n=1.$



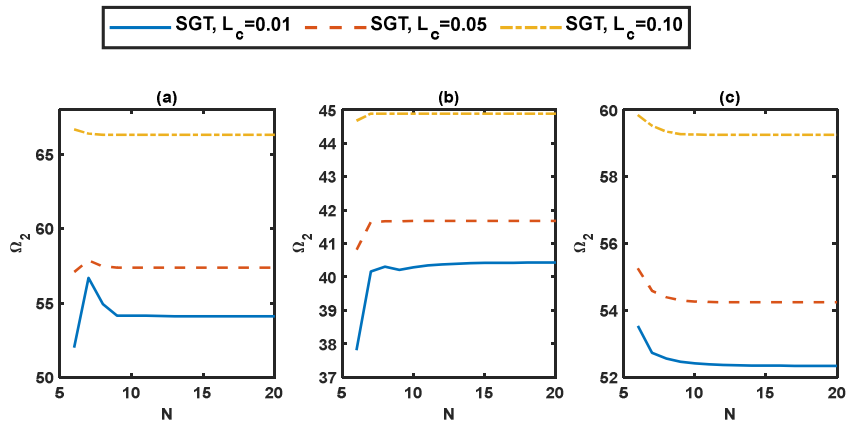


Fig. 4. Evaluating the convergence of the second mode for (a) clamped, (b) simply-supported, and (c) free BCs for $h/R=0.01$, $\nu=0.33$, and $n=1$.

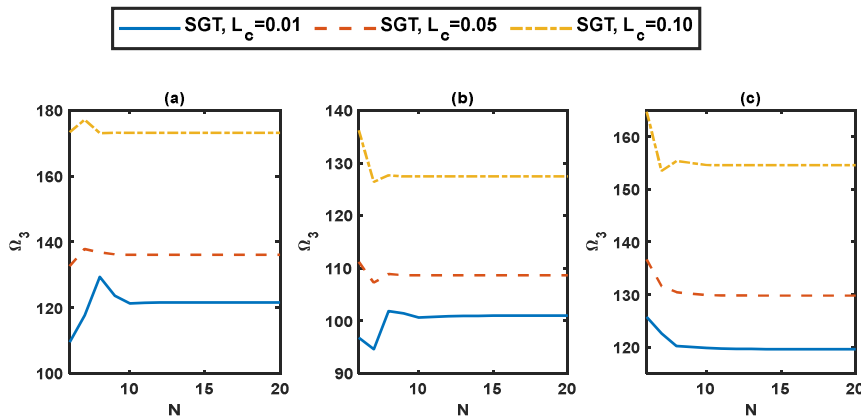


Fig. 5. Evaluating the convergence of the third mode for (a) clamped, (b) simply-supported, and (c) free BCs for $h/R=0.01$, $\nu=0.33$, and $n=1$.

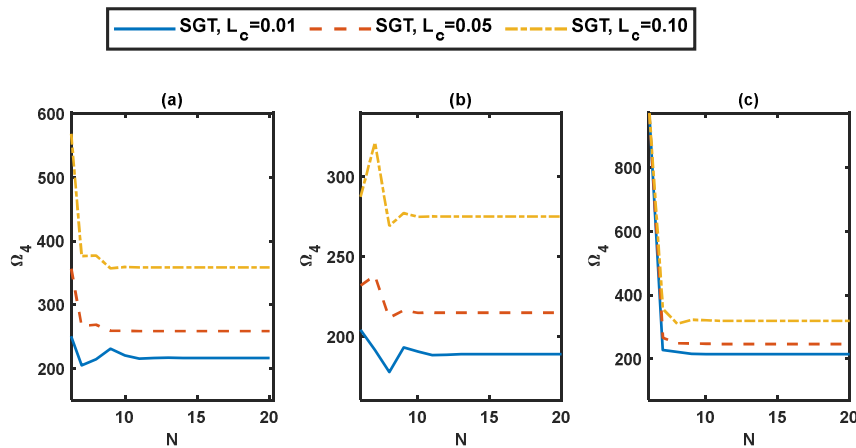


Fig. 6. Evaluating the convergence of the fourth mode for (a) clamped, (b) simply-supported, and (c) free BCs for $h/R=0.01$, $\nu=0.33$, and $n=1$.

Similarly, to evaluate the convergence of GRWM, the first four axisymmetric natural frequencies of the circular nano-plate with clamped, simply-supported, and free B. Cs, based on the NSG, model are presented in Tables 7 to 9 for different values of n , λ , and L_c . The results are extracted based on the functions attained from the SG model and kernel function given in eq. (53).

$$\varphi_\lambda(s, \rho) = \frac{1}{2\lambda} \exp\left(-\frac{|s-\rho|}{\lambda}\right) \tag{53}$$

As can be observed from Tables 7-9, good convergence is obtained.

8. Results and discussions

According to the governing equations of motion for the circular nano-plate (given in eqs. (30-1) and (30-2)), that were obtained based on the non-local SG model, the non-local size parameter λ , material size parameter L_c , heterogeneity index n , aspect ratio h/R , and different B. Cs appeared to be the influential parameters on the vibrational behavior of the structure. To investigate the effects of these parameters, the first dimensionless axisymmetric natural frequencies of the circular nano-plate were extracted for different values of h/R , λ , L_c , n , different B. Cs, and material properties given in Table 10.



Table 7. Convergence evaluation of the first four dimensionless axisymmetric natural frequencies of the circular nano-plate with clamped B.C., based on the NSG model and GWRM for different values of n , λ , and L_c .

n	λ	N_m	Ω_1		Ω_2		Ω_3		Ω_4	
			$L_c=0.05$	$L_c=0.10$	$L_c=0.05$	$L_c=0.10$	$L_c=0.05$	$L_c=0.10$	$L_c=0.05$	$L_c=0.10$
0	0.05	1	10.344	10.931	40.823	47.721	91.567	116.259	163.455	226.569
		2	10.334	10.901	40.628	46.928	91.615	116.514	163.321	226.290
		4	10.335	10.902	40.644	46.947	91.721	116.653	163.698	226.825
		6	10.335	10.902	40.644	46.947	91.721	116.653	163.698	226.825
	0.1	1	10.078	10.629	36.592	42.233	74.802	95.076	121.938	169.037
		2	10.079	10.630	36.609	42.253	74.895	95.193	121.943	168.930
		4	10.081	10.632	36.654	42.308	75.120	95.489	122.546	169.799
		6	10.081	10.632	36.654	42.308	75.120	95.489	122.546	169.799
1	0.05	1	14.023	14.793	55.126	63.674	124.262	158.043	221.824	307.478
		2	14.023	14.793	55.134	63.684	124.333	158.125	221.664	307.129
		4	14.024	14.794	55.158	63.712	124.490	158.330	222.224	307.924
		6	14.024	14.794	55.158	63.712	124.490	158.330	222.224	307.924
	0.1	1	13.677	14.424	49.659	57.314	101.523	129.039	165.505	229.435
		2	13.678	14.426	49.685	57.345	101.659	129.212	165.548	229.338
		4	13.681	14.429	49.752	57.425	101.993	129.652	166.440	230.628
		6	13.681	14.429	49.752	57.425	101.993	129.652	166.440	230.628

Table 8. Convergence evaluation of the first four dimensionless axisymmetric natural frequencies of the circular nano-plate with simply supported B.C., based on the NSG model and GWRM for different values of n , λ , and L_c .

n	λ	N_m	Ω_1		Ω_2		Ω_3		Ω_4	
			$L_c=0.05$	$L_c=0.10$	$L_c=0.05$	$L_c=0.10$	$L_c=0.05$	$L_c=0.10$	$L_c=0.05$	$L_c=0.10$
0	0.05	1	4.971	5.030	29.613	31.888	73.534	86.207	136.448	174.550
		2	4.972	5.030	29.617	31.891	73.563	86.232	136.607	174.779
		4	4.972	5.030	29.625	31.898	73.626	86.300	136.861	175.091
		6	4.972	5.030	29.625	31.898	73.626	86.300	136.861	175.091
	0.1	1	4.868	4.926	26.903	28.962	60.634	71.019	102.557	131.038
		2	4.869	4.926	26.913	28.971	60.692	71.076	102.771	131.320
		4	4.869	4.926	26.935	28.993	60.829	71.229	103.188	131.840
		6	4.869	4.926	26.935	28.993	60.829	71.229	103.188	131.840
1	0.05	1	6.746	6.826	40.185	43.273	99.789	116.986	185.170	236.878
		2	6.747	6.826	40.192	43.277	99.832	117.023	185.400	237.205
		4	6.747	6.826	40.203	43.288	99.925	117.125	185.776	237.666
		6	6.747	6.826	40.203	43.288	99.925	117.125	185.776	237.666
	0.1	1	6.606	6.684	36.510	39.303	82.290	96.383	139.195	177.851
		2	6.607	6.684	36.524	39.316	82.375	96.469	139.509	178.261
		4	6.607	6.685	36.556	39.349	82.579	96.695	140.125	179.031
		6	6.607	6.685	36.556	39.349	82.579	96.695	140.125	179.031

Table 9. Convergence evaluation of the first four dimensionless axisymmetric natural frequencies of the circular nano-plate with free-edge B.C., based on the NSG model and GWRM for different values of n , λ , and L_c .

n	λ	N_m	Ω_1		Ω_2		Ω_3		Ω_4	
			$L_c=0.05$	$L_c=0.10$	$L_c=0.05$	$L_c=0.10$	$L_c=0.05$	$L_c=0.10$	$L_c=0.05$	$L_c=0.10$
0	0.05	1	9.078	9.241	38.533	42.198	87.910	105.348	157.563	206.460
		2	9.077	9.241	38.524	42.201	87.903	105.383	157.109	205.443
		4	9.077	9.241	38.535	42.214	87.997	105.498	157.448	205.946
		6	9.077	9.241	38.535	42.214	87.997	105.498	157.448	205.946
	0.1	1	8.906	9.077	34.959	38.537	72.517	87.963	118.915	158.106
		2	8.905	9.078	34.964	38.551	72.580	88.063	118.692	157.430
		4	8.907	9.079	35.000	38.590	72.797	88.325	119.249	158.218
		6	8.907	9.079	35.000	38.590	72.797	88.325	119.249	158.218
1	0.05	1	12.319	12.540	52.290	57.264	119.300	142.964	213.826	280.184
		2	12.317	12.540	52.279	57.269	119.295	143.017	213.229	278.826
		4	12.318	12.540	52.295	57.288	119.435	143.188	213.729	279.560
		6	12.318	12.540	52.295	57.288	119.435	143.188	213.729	279.560
	0.1	1	12.086	12.318	47.443	52.298	98.422	119.385	161.399	214.593
		2	12.085	12.319	47.451	52.318	98.518	119.534	161.127	213.713
		4	12.087	12.321	47.504	52.377	98.840	119.922	161.949	214.873
		6	12.087	12.321	47.504	52.377	98.840	119.922	161.949	214.873

Table 10. Mechanical properties of circular nano-plate.

E_c (Gpa)	E_m (Gpa)	ρ_c (Kg/m ³)	ρ_m (Kg/m ³)	ν	N_m
380	211	3600	7860	0.33	4



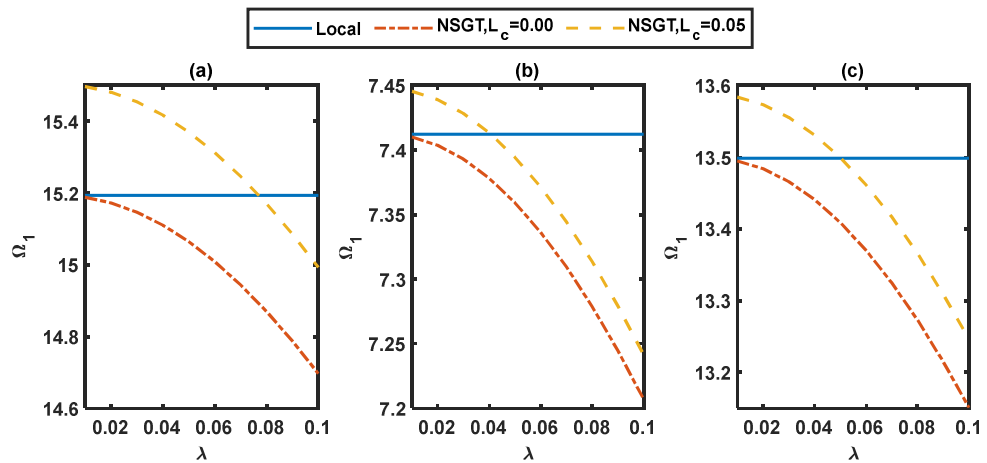


Fig. 7. Evaluating the influence of λ on the first dimensionless axisymmetric natural frequency of circular nano-plate with (a) clamped, (b) simply-supported and (c) free BCs for $h/R=0.01$, $\nu=0.33$ and $n=2$.

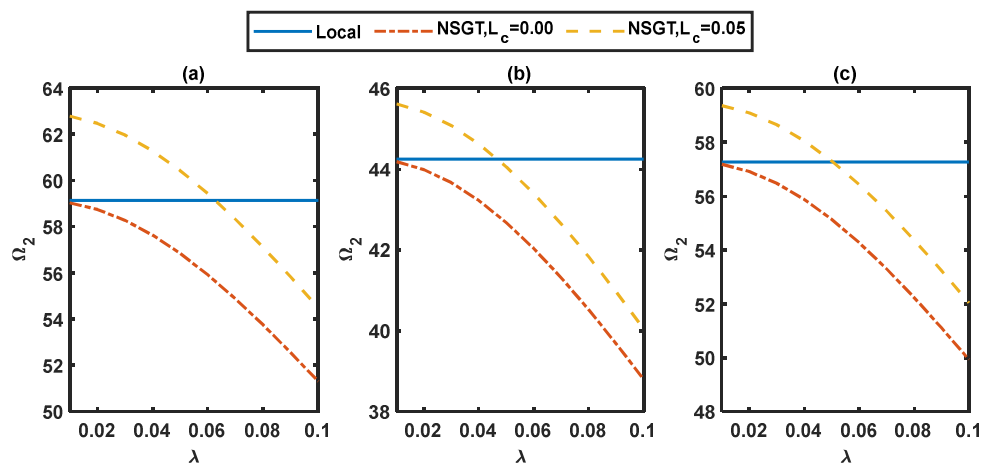


Fig. 8. Influence of λ on the second dimensionless axisymmetric natural frequency of the circular nano-plate with (a) clamped, (b) simply-supported and (c) free BCs for $h/R=0.01$, $\nu=0.33$ and $n=2$.

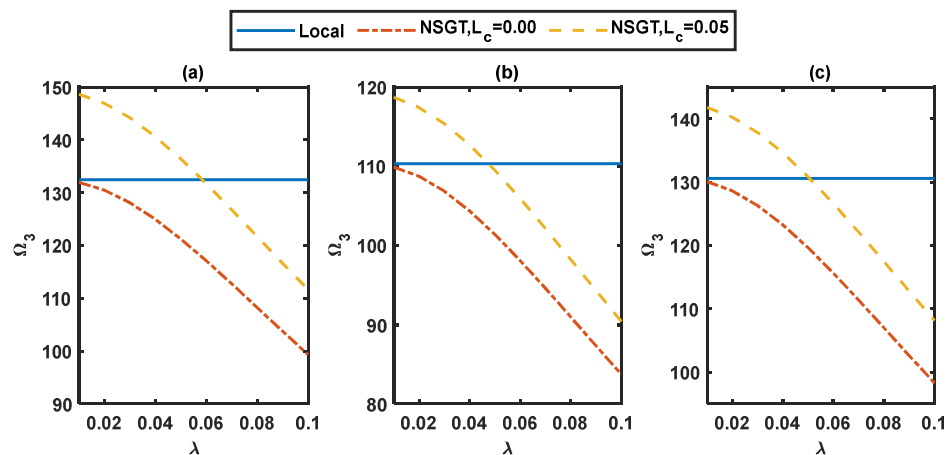


Fig. 9. Influence of λ on the third dimensionless axisymmetric natural frequency of the circular nano-plate with (a) clamped, (b) simply-supported and (c) free BCs for $h/R=0.01$, $\nu=0.33$ and $n=2$.

8.1. Effect of non-local parameter λ and BCs on the vibrational behavior

In this section, the influence of λ and BCs on the vibrational characteristics of the circular nano-plate are assessed. For this purpose, the first four dimensionless natural frequencies of a nano-plate with clamped, simply-supported, and free-edge BCs, based on the NSG model, are plotted against the non-local parameter of λ in Figs. 7 to 10. According to these figures, increasing λ produces a decreasing trend in the frequency ratio in all modes, for all postulated BCs and L_c . This indicates that this parameter leads to a softening behavior on the plate vibrational behavior. The highest and lowest decreasing rates in the natural frequencies were associated with the clamped and simply-supported BCs, respectively. Additionally, the highest increase in the frequency ratio was related to the fourth mode; while the lowest increase was related to the first mode. Also, sharper decreasing trends were observed for the first to the fourth modes.



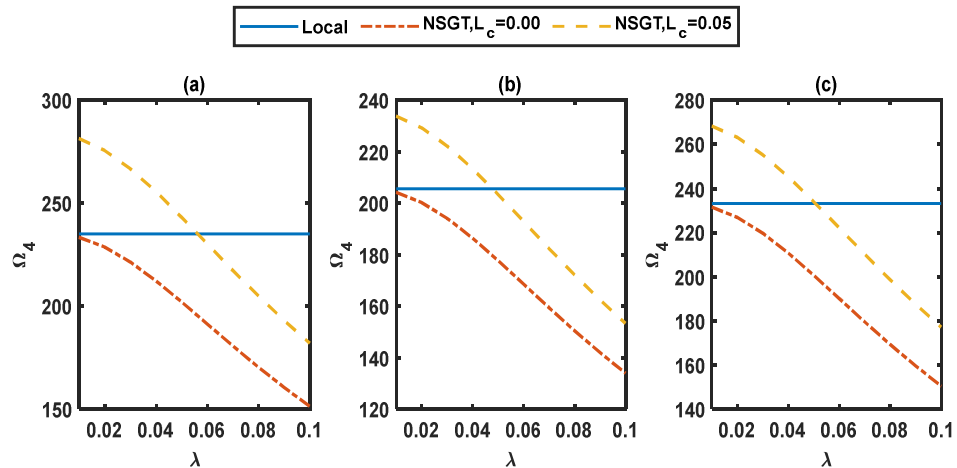


Fig. 10. Influence of λ on the fourth dimensionless axisymmetric natural frequency of the circular nano-plate with (a) clamped, (b) simply-supported and (c) free BCs for $h/R=0.01$, $\nu=0.33$ and $n=2$.

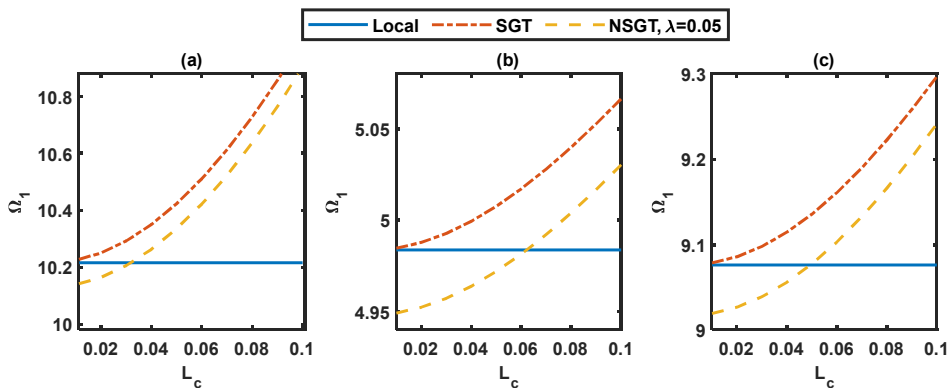


Fig. 11. Influence of L_c on the first dimensionless axisymmetric natural frequency of the circular nano-plate with (a) clamped, (b) simply-supported and (c) free BCs for $h/R=0.01$, $\nu=0.33$ and $n=0$.

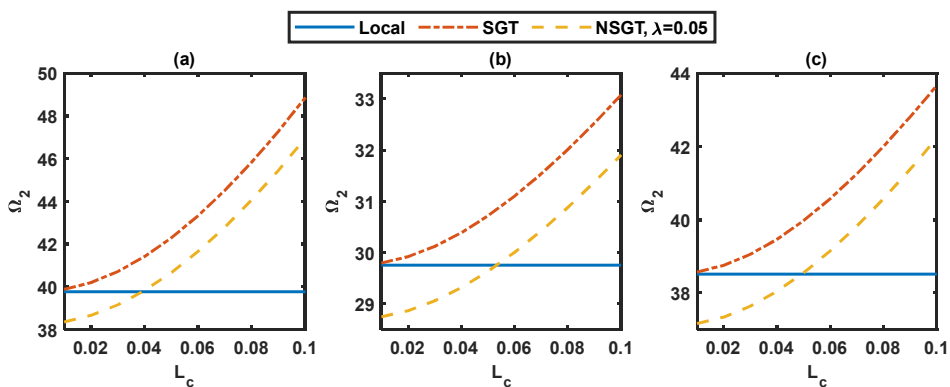


Fig. 12. Influence of L_c on the second dimensionless axisymmetric natural frequency of the circular nano-plate with (a) clamped, (b) simply-supported, and (c) free BCs for $h/R=0.01$, $\nu=0.33$, and $n=0$.

8.2. Effect of material size parameter L_c and BCs on the vibrational behavior

This section is devoted to the influence of material size parameter L_c as well as BCs on the vibrational characteristics of the circular nano-plate. Accordingly, the first four dimensionless natural frequencies with clamped, simply-supported and free-edge BCs obtained from the NSG model were plotted against material size parameter L_c , as shown in Figs. 11 to 17. According to these figures, an increasing trend in frequency ratio is observed in all modes and BCs as L_c is increased. This indicates that based on the strain gradient theory the increase in this parameter leads to a stiffer plate. The highest and lowest increase rates were associated with the clamped and simply-supported BCs. In addition, the highest increase in the frequency ratio was related to the fourth mode while the lowest decrease was associated with the first mode.



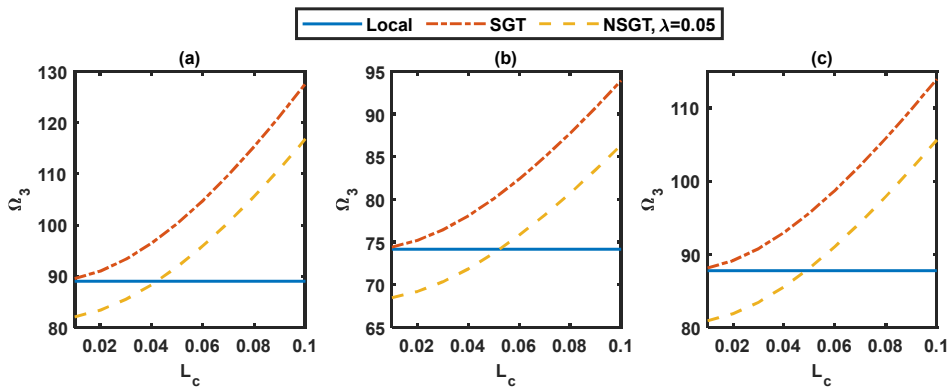


Fig. 13. Influence of L_c on the third dimensionless axisymmetric natural frequency of the circular nano-plate with (a) clamped, (b) simply-supported, and (c) free BCs for $h/R=0.01$, $\nu=0.33$, and $n=0$.

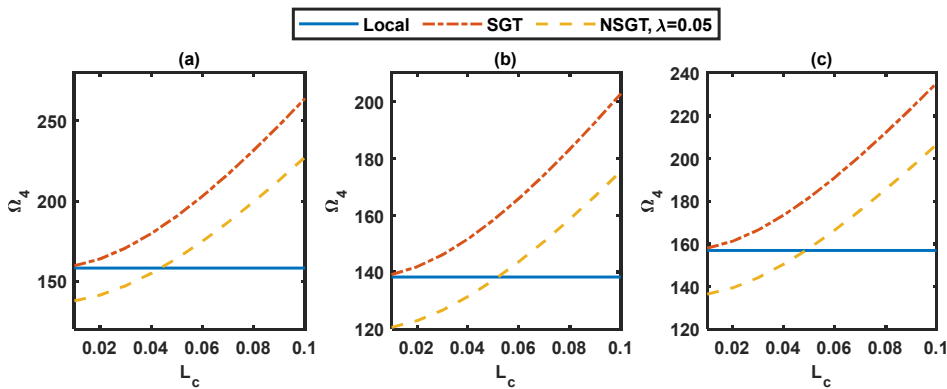


Fig. 14. Influence of L_c on the fourth dimensionless axisymmetric natural frequency of the circular nano-plate with (a) clamped, (b) simply-supported, and (c) free BCs for $h/R=0.01$, $\nu=0.33$, and $n=0$.

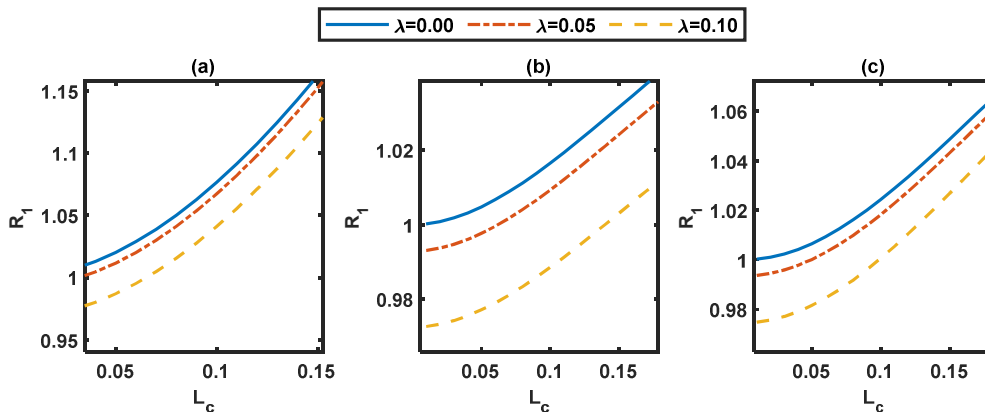


Fig. 15. The effect of λ , L_c , and BCs on the dimensionless natural frequency ratio of the first mode, a) clamped, (b) simply-supported, and (c) free edge BCs with $h/R=0.01$, $\nu=0.33$, and $n=1$.

8.3. The effects of size parameter L_c and the non-local parameter λ on the vibrational behavior

This section investigates the influence of size parameter L_c , non-local parameter λ , and BCs on the vibrational behavior of the circular nano-plate. Accordingly, the variations in frequency ratio, $R_i = \Omega_{i,Nonlocal} / \Omega_{i,local}$, based on the NSG model, are shown in terms of L_c and λ for clamped, simply-supported, and free-edge B. Cs Fig. 16 to 19. According to Figs. 15 to 18, increasing L_c results in an increase in the frequency ratio in all modes and all used B. Cs. This indicates that this parameter has a stiffening effect on the vibration behavior of the nano-plate. The highest increasing rate in the frequency ratio was associated with the clamped BCs, while the simply-supported BCs. attained the lowest rate of increase. Moreover, the first and fourth modes had the lowest and highest increase in the frequency ratio, respectively. Results in Figs. 15 to 18 indicate that the increase in λ leads to a decrease in the frequency ratio for all types of BCs, in all modes. This indicates that based on the non-local model, this parameter appears to have a softening effect on the plate vibrational behavior. The highest and lowest decreases in the frequency ratios were associated with the fourth and first modes, respectively.



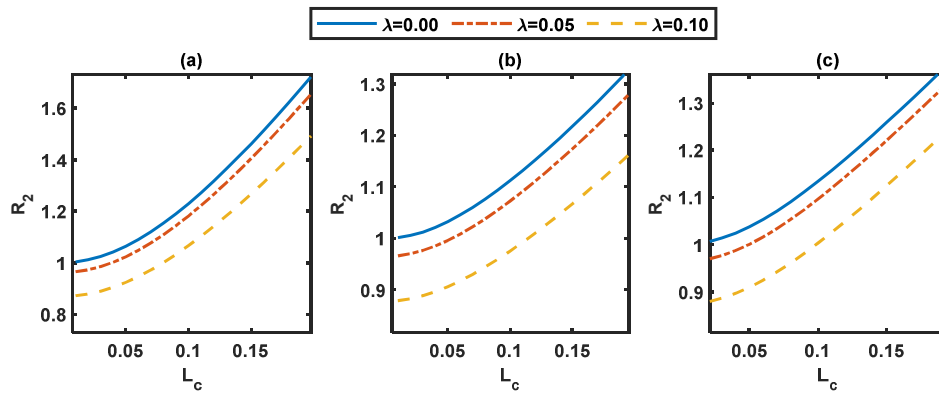


Fig. 16. The effect of λ , L_c , and BCs on the dimensionless natural frequency ratio of the second mode, a) clamped, (b) simply-supported, and (c) free edge BCs with $h/R=0.01$, $\nu=0.33$, and $n=1$.

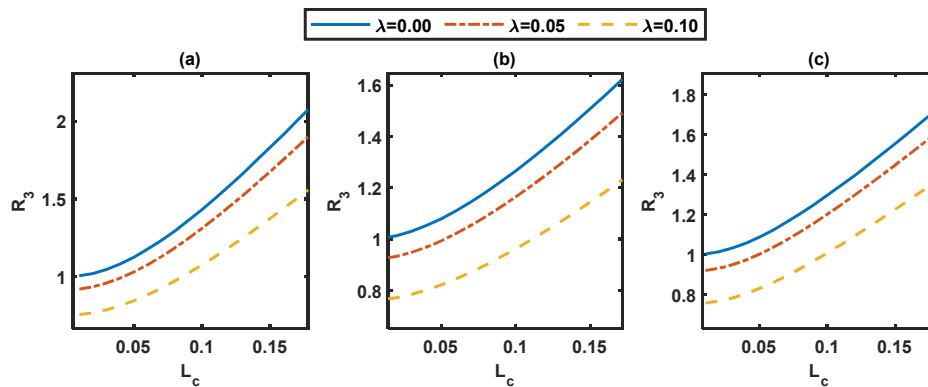


Fig. 17. The effect of λ , L_c , and B. Cs on the dimensionless natural frequency ratio of the third mode, a) clamped, (b) simply-supported, and (c) free edge BCs with $h/R=0.01$, $\nu=0.33$, and $n=1$.

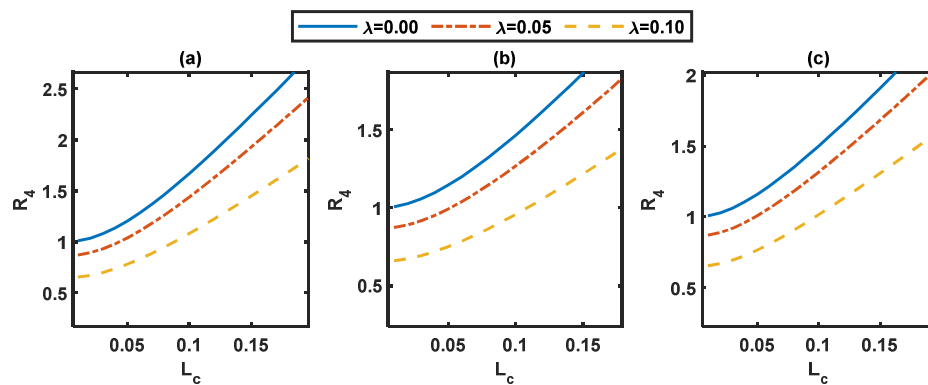


Fig. 18. The effect of λ , L_c , and B. Cs on the dimensionless natural frequency ratio of the fourth mode, a) clamped, (b) simply-supported, and (c) free edge BCs with $h/R=0.01$, $\nu=0.33$, and $n=1$.

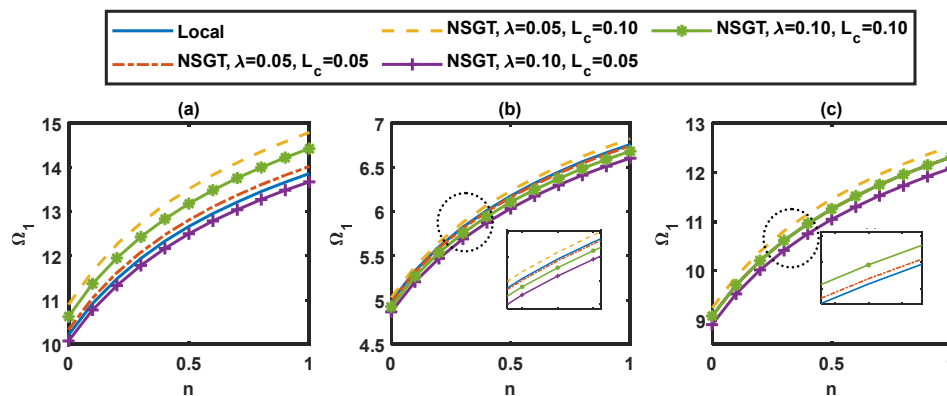


Fig. 19. The effect of n , L_c and λ on the natural frequency of the first mode, (a) clamped, (b) simply-supported, and (c) free-edge condition with $h/R=0.01$, $\nu=0.33$, and $n=1$.



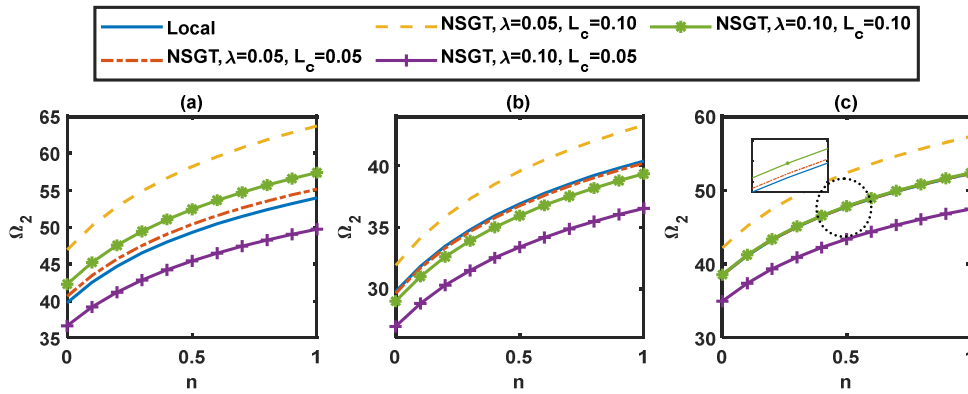


Fig. 20. The effect of n , L_c and λ on the natural frequency of the second mode, (a) clamped, (b) simply-supported, and (c) free-edge condition with $h/R=0.01$, $\nu=0.33$, and $n=1$.

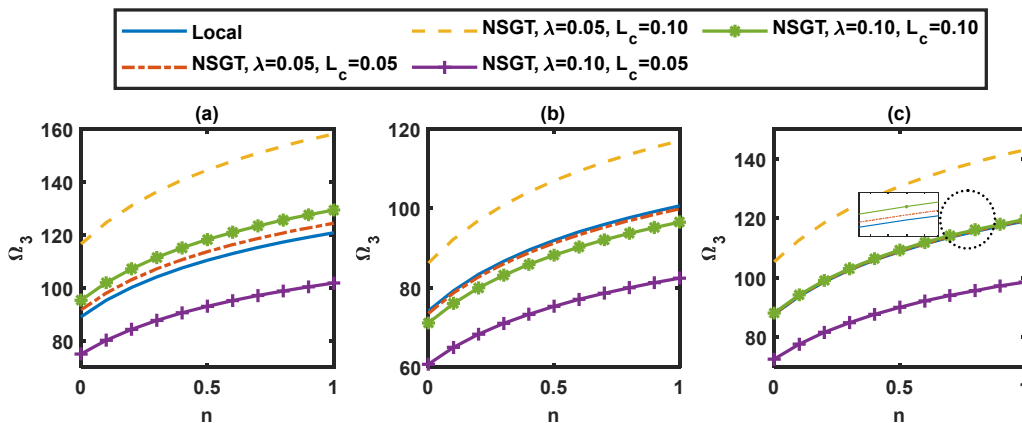


Fig. 21. The effect of n , L_c and λ on the natural frequency of the third mode, (a) clamped, (b) simply-supported, and (c) free-edge condition with $h/R=0.01$, $\nu=0.33$, and $n=1$.

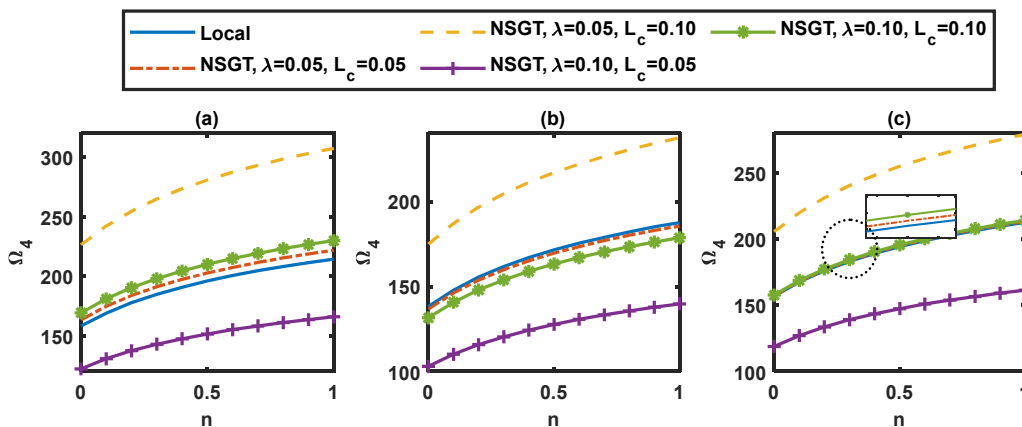


Fig. 22. The effect of n , L_c and λ on the natural frequency of the fourth mode, (a) clamped, (b) simply-supported, and (c) free-edge condition with $h/R=0.01$, $\nu=0.33$, and $n=1$.

8.4. The effect of heterogeneous index n on the vibration behavior

According to the presented results in Figs. 19 to 22, the increase in the heterogeneity index parameter n is followed by an increase in the natural frequency of the circular nano-plate for all BCs. The increasing rate is more pronounced at larger values of the non-local parameter. The highest increase in the natural frequency was associated with the clamped BCs, while the simply-supported and free BCs experience approximately the same trends. Increasing L_c and n , increased the frequency, for all types of BCs and modes. Decreasing λ and n , increased the frequency value in all modes and all types of BCs.

9. Conclusions

In this paper, a new methodology for solving the linear free-vibration of a circular nano-plate was formulated by applying Hamilton's principle, based on the NSG model in the integral form. The proposed model had two independent size parameters that could lead to a softening or stiffening effect for the nano-plate. Considering $L_c=\lambda=0$, the derived governing equations were reduced to those represented by the local elasticity theory. To seek a solution, the derived governing equations, in the integral form, were transformed to differential forms. However, the integral forms of the governing equations were solved directly using the specified Kerl function. The obtained governing equations were solved using the application of GDQR and GWRM methods



based on different BCs, which included clamped, simply-supported, and free-edge. Results, as well as the solution method, show that the proposed methodology seems to be straightforward, useful, and a powerful technique for modeling the nano-structure such as plates. In addition, the proposed solution method is appropriate for analyzing the linear vibrational phenomena when the size effect is included. Moreover, results show an increase in the frequency ratio for all types of introduced BCs and modes when the material size parameter L_c increases. This means that the presence of this parameter leads to a stiffening behavior for the vibrational behavior of the nano-plate. Moreover, the highest increasing rate of frequency ratio was achieved for the clamped BC, while the lowest rate was associated with the simply-supported edge. Additionally, the highest and lowest increases in the frequency ratio were attributed to the fourth and first modes, respectively. Additionally, it was shown that for all types of BCs and modes, the increase in non-local parameter λ was followed by a decrease in the frequency ratio. This means that the presence of this parameter leads to a softening behavior for the nano-plate. Finally, the highest decrease in frequency ratio was related to the fourth mode while the lowest decrease was associated with the first mode.

Author Contributions

M. Pourabdy planned the scheme, initiated the project, and suggested the experiments; M. Shishehsaz conducted the experiments and analyzed the empirical results; S. Shahrooi and S.A.S. Roknizadeh developed the mathematical modeling and examined the theory validation. The manuscript was written through the contribution of all authors. All authors discussed the results, reviewed, and approved the final version of the manuscript.

Conflict of Interest

The authors declared no potential conflicts of interest concerning the research, authorship, and publication of this article.

Funding

The authors received no financial support for the research, authorship, and publication of this article.

Data Availability Statements

The datasets generated and/or analyzed during the current study are available from the corresponding author on reasonable request.

Nomenclature

E	Elastic modulus [GPa]	$\sigma_{rr}, \sigma_{\theta\theta}$	Components of stress tensor along r and θ axes
ρ	Density [Kg/m ³]	$\varphi_{\text{eqa}}, \varphi_{\lambda}$	Kernel function
ν	Poisson's ratio	ℓ_s, L_c	The dimensional and non-dimensional material size parameter
n	Heterogeneity index of the FG material	$e_0 a, \lambda$	The dimensional and non-dimensional non-local size parameter
m	Indices specify the metal phases of FG material	ω_n	Natural frequency
c	Indices specify the ceramic phases of FG material	Ω_n	Dimensionless natural frequency
V	Volume ratio	$L(x)$	Legendre interpolation function
u_r, u_z	Radial and transverse components of the displacement field	$\{U_b\}, \{W_b\}$	Mode shapes
u_0, w_0	Displacement functions along the radial and transverse axes of the nano-plate mid-plane	N_m	Number of modes
A, B, D	Elastic constants of the circular nano-plate	I_0, I_1, I_2	Inertial constants
$\varepsilon_{rr}^0, \varepsilon_{\theta\theta}^0$	Normal strain components of the mid-plane along r and θ axes	$\sigma_{rr}^{(0)}, \sigma_{\theta\theta}^{(0)}$	Zero-order of stress components in the SG model
$\kappa_{rr}, \kappa_{\theta\theta}$	The curvature of the nano-plate along r and θ axes	$\sigma_{rr}^{(1)}, \sigma_{\theta\theta}^{(1)}$	First order of stress components in the SG model
$N_{rr}, N_{\theta\theta}$	Stress resultant force along r and θ axes	$\varepsilon_{rrr}, \varepsilon_{\theta\theta r}, \varepsilon_{r\theta\theta}$	First order of strain components in the SG model
$M_{rr}, M_{\theta\theta}$	Stress resultant moment along r and θ axes		

References

- [1] P. Ball, "Roll up for the revolution," ed: Nature Publishing Group, 2001.
- [2] R. H. Baughman, A. A. Zakhidov, and W. A. De Heer, "Carbon nanotubes--the route toward applications," *science*, vol. 297, pp. 787-792, 2002.
- [3] B. Bodily and C. Sun, "Structural and equivalent continuum properties of single-walled carbon nanotubes," *International Journal of Materials and Product Technology*, vol. 18, pp. 381-397, 2003.
- [4] C. Li and T.-W. Chou, "A structural mechanics approach for the analysis of carbon nanotubes," *International Journal of Solids and Structures*, vol. 40, pp. 2487-2499, 2003.
- [5] C. Li and T.-W. Chou, "Single-walled carbon nanotubes as ultrahigh frequency nanomechanical resonators," *Physical review B*, vol. 68, p. 073405, 2003.
- [6] S. Pradhan and J. Phadikar, "Nonlinear analysis of carbon nanotubes, Proceedings of Fifth International Conference on Smart Materials," *Structures and Systems, Indian Institute of Science, Bangalore*, pp. 24-26, 2008.
- [7] A. Chong, F. Yang, D. C. Lam, and P. Tong, "Torsion and bending of micron-scaled structures," *Journal of Materials Research*, vol. 16, pp. 1052-1058, 2001.
- [8] N. Fleck, G. Muller, M. Ashby, and J. Hutchinson, "Strain gradient plasticity: theory and experiment," *Acta Metallurgica et Materialia*, vol. 42, pp. 475-487, 1994.
- [9] A. C. Eringen, "On differential equations of nonlocal elasticity and solutions of screw dislocation and surface waves," *Journal of applied physics*, vol. 54, pp. 4703-4710, 1983.
- [10] A. C. Eringen, "Linear theory of nonlocal elasticity and dispersion of plane waves," *International Journal of Engineering Science*, vol. 10, pp. 425-435, 1972.




- [11] M. Shishesaz, M. Shariati, and A. Yaghootian, "Nonlocal Elasticity Effect on Linear Vibration of Nano-circular Plate Using Adomian Decomposition Method," *Journal of Applied and Computational Mechanics*, vol. 6, pp. 63-76, 2020.
- [12] M. Shishesaz, M. Shariati, A. Yaghootian, and A. Alizadeh, "Nonlinear Vibration Analysis of Nano-Disks Based on Nonlocal Elasticity Theory Using Homotopy Perturbation Method," *International Journal of Applied Mechanics*, vol. 11, p. 1950011, 2019.
- [13] H. Bakhshalizadeh and M. Ghadiri, "Size-dependent vibration behavior of graphene sheet with attached spring-mass and damper system based on the nonlocal Eringen theory," *Mechanics of Advanced Materials and Structures*, pp. 1-10, 2020.
- [14] M. Ghadiri and N. Shafiei, "Vibration analysis of a nano-turbine blade based on Eringen nonlocal elasticity applying the differential quadrature method," *Journal of Vibration and Control*, vol. 23, pp. 3247-3265, 2017.
- [15] E. Mohammad-Rezaei Bidgoli and M. Arefi, "Free vibration analysis of micro plate reinforced with functionally graded graphene nanoplatelets based on modified strain-gradient formulation," *Journal of Sandwich Structures & Materials*, vol. 23, pp. 436-472, 2021.
- [16] A. Timoshin, A. Kazemi, M. H. Beni, J. E. Jam, and B. Pham, "Nonlinear strain gradient forced vibration analysis of shear deformable microplates via hermitian finite elements," *Thin-Walled Structures*, vol. 161, p. 107515, 2021.
- [17] B. Zhang, H. Li, L. Kong, H. Shen, and X. Zhang, "Coupling effects of surface energy, strain gradient, and inertia gradient on the vibration behavior of small-scale beams," *International Journal of Mechanical Sciences*, vol. 184, p. 105834, 2020.
- [18] A. Assadi, "Size dependent forced vibration of nanoplates with consideration of surface effects," *Applied Mathematical Modelling*, vol. 37, pp. 3575-3588, 2013.
- [19] F. Ebrahimi and M. R. Barati, "Surface effects on the vibration behavior of flexoelectric nanobeams based on nonlocal elasticity theory," *The European Physical Journal Plus*, vol. 132, pp. 1-13, 2017.
- [20] A. Norouzzadeh and R. Ansari, "Isogeometric vibration analysis of functionally graded nanoplates with the consideration of nonlocal and surface effects," *Thin-Walled Structures*, vol. 127, pp. 354-372, 2018.
- [21] S. Esfahani, S. E. Khadem, and A. E. Mamaghani, "Nonlinear vibration analysis of an electrostatic functionally graded nano-resonator with surface effects based on nonlocal strain gradient theory," *International Journal of Mechanical Sciences*, vol. 151, pp. 508-522, 2019.
- [22] M. A. Alazwari, A. A. Abdelrahman, A. Wagih, M. A. Eltaher, and H. E. Abd-El-Mottaleb, "Static analysis of cutout microstructures incorporating the microstructure and surface effects," *Steel and Composite Structures*, vol. 38, pp. 583-597, 2021.
- [23] A. Assadi and M. Nazemizadeh, "Size-dependent Vibration Analysis of Stepped Nanobeams Based on Surface Elasticity Theory," *International Journal of Engineering*, vol. 34, pp. 744-749, 2021.
- [24] S. Behdad, M. Fakher, and S. Hosseini-Hashemi, "Dynamic stability and vibration of two-phase local/nonlocal VFGP nanobeams incorporating surface effects and different boundary conditions," *Mechanics of Materials*, vol. 153, p. 103633, 2021.
- [25] A. E. Abouelregal and W. W. Mohammed, "Effects of nonlocal thermoelasticity on nanoscale beams based on couple stress theory," *Mathematical Methods in the Applied Sciences*, 2020.
- [26] M. Akbarzadeh Khorshidi and D. Soltani, "Nanostructure-dependent dispersion of carbon nanostructures: New insights into the modified couple stress theory," *Mathematical Methods in the Applied Sciences*, 2020.
- [27] M. Al-Furjan, E. Samimi-Sohrforozani, M. Habibi, D. won Jung, and H. Safarpour, "Vibrational characteristics of a higher-order laminated composite viscoelastic annular microplate via modified couple stress theory," *Composite Structures*, vol. 257, p. 113152, 2021.
- [28] H. Babaei and M. R. Eslami, "Size-dependent vibrations of thermally pre/post-buckled FG porous micro-tubes based on modified couple stress theory," *International Journal of Mechanical Sciences*, vol. 180, p. 105694, 2020.
- [29] M. A. Khorshidi, "Validation of weakening effect in modified couple stress theory: dispersion analysis of carbon nanotubes," *International Journal of Mechanical Sciences*, vol. 170, p. 105358, 2020.
- [30] H. Kumar and S. Mukhopadhyay, "Thermoelastic damping analysis for size-dependent microplate resonators utilizing the modified couple stress theory and the three-phase-lag heat conduction model," *International Journal of Heat and Mass Transfer*, vol. 148, p. 118997, 2020.
- [31] M. Najafzadeh, M. M. Adeli, E. Zarezadeh, and A. Hadi, "Torsional vibration of the porous nanotube with an arbitrary cross-section based on couple stress theory under magnetic field," *Mechanics Based Design of Structures and Machines*, pp. 1-15, 2020.
- [32] A. Apuzzo, C. Bartolomeo, R. Luciano, and D. Scorza, "Novel local/nonlocal formulation of the stress-driven model through closed form solution for higher vibrations modes," *Composite Structures*, vol. 252, p. 112688, 2020.
- [33] H. M. Sedighi and M. J. P. S. Malikan, "Stress-driven nonlocal elasticity for nonlinear vibration characteristics of carbon/boron-nitride hetero-nanotube subject to magneto-thermal environment," vol. 95, p. 055218, 2020.
- [34] X. Yang, S. Sahmani, and B. Safaei, "Postbuckling analysis of hydrostatic pressurized FGM microsized shells including strain gradient and stress-driven nonlocal effects," *Engineering with Computers*, 2020/01/02 2020.
- [35] A. A. Abdelrahman, I. Esen, C. Özarpa, and M. A. Eltaher, "Dynamics of perforated nanobeams subject to moving mass using the nonlocal strain gradient theory," *Applied Mathematical Modelling*, vol. 96, pp. 215-235, 2021.
- [36] M. Al-Furjan, R. Dehini, M. Khorami, M. Habibi, and D. won Jung, "On the dynamics of the ultra-fast rotating cantilever orthotropic piezoelectric nanodisk based on nonlocal strain gradient theory," *Composite Structures*, vol. 255, p. 112990, 2021.
- [37] R. Barretta, S. A. Faghidian, and F. M. de Sciarra, "Stress-driven nonlocal integral elasticity for axisymmetric nano-plates," *International Journal of Engineering Science*, vol. 136, pp. 38-52, 2019.
- [38] A. A. Daikh, M. S. A. Houari, and M. A. Eltaher, "A novel nonlocal strain gradient Quasi-3D bending analysis of sigmoid functionally graded sandwich nanoplates," *Composite Structures*, vol. 262, p. 113347, 2021.
- [39] C. Lim, G. Zhang, and J. Reddy, "A higher-order nonlocal elasticity and strain gradient theory and its applications in wave propagation," *Journal of the Mechanics and Physics of Solids*, vol. 78, pp. 298-313, 2015.
- [40] G. T. Monaco, N. Fantuzzi, F. Fabbrocino, and R. Luciano, "Hygro-thermal vibrations and buckling of laminated nanoplates via nonlocal strain gradient theory," *Composite Structures*, vol. 262, p. 113337, 2021.
- [41] C. H. Thai, A. Ferreira, and P. Phung-Van, "A nonlocal strain gradient isogeometric model for free vibration and bending analyses of functionally graded plates," *Composite Structures*, vol. 251, p. 112634, 2020.
- [42] P. T. Thang, P. Tran, and T. Nguyen-Thoi, "Applying nonlocal strain gradient theory to size-dependent analysis of functionally graded carbon nanotube-reinforced composite nanoplates," *Applied Mathematical Modelling*, vol. 93, pp. 775-791, 2021.
- [43] J. Torabi, R. Ansari, A. Zabihi, and K. Hosseini, "Dynamic and pull-in instability analyses of functionally graded nanoplates via nonlocal strain gradient theory," *Mechanics Based Design of Structures and Machines*, pp. 1-21, 2020.
- [44] W.-s. Xiao and P. Dai, "Static analysis of a circular nanotube made of functionally graded bi-semi-tubes using nonlocal strain gradient theory and a refined shear model," *European Journal of Mechanics-A/Solids*, vol. 82, p. 103979, 2020.
- [45] A. Zenkour and A. Radwan, "A compressive study for porous FG curved nanobeam under various boundary conditions via a nonlocal strain gradient theory," *The European Physical Journal Plus*, vol. 136, pp. 1-16, 2021.
- [46] M. Zarei, G. Faghani, M. Ghalami, and G. H. Rahimi, "Buckling and vibration analysis of tapered circular nano plate," *Journal of Applied and Computational Mechanics*, vol. 4, pp. 40-54, 2018.
- [47] A. Li, X. Ji, S. Zhou, L. Wang, J. Chen, and P. Liu, "Nonlinear axisymmetric bending analysis of strain gradient thin circular plate," *Applied Mathematical Modelling*, vol. 89, pp. 363-380, 2021.
- [48] Q. Luo, C. Li, and S. Li, "Transverse Free Vibration of Axisymmetric Functionally Graded Circular Nanoplates with Radial Loads," *Journal of Vibration Engineering & Technologies*, pp. 1-16, 2021.
- [49] Y. Yang, Z.-L. Hu, and X.-F. Li, "Axisymmetric bending and vibration of circular nanoplates with surface stresses," *Thin-Walled Structures*, vol. 166, p. 108086, 2021.
- [50] S. A. Faghidian, "Higher order mixture nonlocal gradient theory of wave propagation," *Mathematical Methods in the Applied Sciences*, 2020.
- [51] S. A. Faghidian, "Higher-order nonlocal gradient elasticity: a consistent variational theory," *International Journal of Engineering Science*, vol. 154, p. 103337, 2020.
- [52] S. A. Faghidian, "Flexure mechanics of nonlocal modified gradient nano-beams," *Journal of Computational Design and Engineering*, vol. 8, pp. 949-959, 2021.
- [53] S. A. Faghidian, "Contribution of nonlocal integral elasticity to modified strain gradient theory," *The European Physical Journal Plus*, vol. 136, pp. 1-18, 2021.
- [54] S. P. Timoshenko and S. Woinowsky-Krieger, *Theory of plates and shells*: McGraw-hill, 1959.





- [55] A. W. Leissa, *Vibration of plates* vol. 160: Scientific and Technical Information Division, National Aeronautics and ..., 1969.
- [56] J. Zhao and D. Pedroso, "Strain gradient theory in orthogonal curvilinear coordinates," *International Journal of Solids and Structures*, vol. 45, pp. 3507-3520, 2008.
- [57] S. A. Faghidian, "A smoothed inverse eigenstrain method for reconstruction of the regularized residual fields," *International Journal of Solids and Structures*, vol. 51, pp. 4427-4434, 2014.
- [58] S. A. Faghidian, "Inverse determination of the regularized residual stress and eigenstrain fields due to surface peening," *The Journal of Strain Analysis for Engineering Design*, vol. 50, pp. 84-91, 2015.
- [59] G. Liu and T. Wu, "Numerical solution for differential equations of duffing-type non-linearity using the generalized differential quadrature rule," *Journal of Sound and Vibration*, vol. 237, pp. 805-817, 2000.
- [60] J. Quan and C. Chang, "New insights in solving distributed system equations by the quadrature method—I. Analysis," *Computers & Chemical Engineering*, vol. 13, pp. 779-788, 1989.
- [61] C. Shu and B. E. Richards, "Application of Generalised Differential Quadrature to Solve Two-Dimensional Incompressible Navier-Stokes Equations. GU Aero Report 9227," 1992.
- [62] X. Ji, A. Li, and S. Zhou, "A comparison of strain gradient theories with applications to the functionally graded circular micro-plate," *Applied Mathematical Modelling*, vol. 49, pp. 124-143, 2017.

ORCID iD

Mortaza Pourabdy  <https://orcid.org/0000-0002-7211-6585>

Mohammad Shishehsaz  <https://orcid.org/0000-0002-1892-1946>

Shahram Shahrooi  <https://orcid.org/0000-0003-3367-6712>

S. Alireza S. Roknizadeh  <https://orcid.org/0000-0002-6731-7956>



© 2021 Shahid Chamran University of Ahvaz, Ahvaz, Iran. This article is an open access article distributed under the terms and conditions of the Creative Commons Attribution-NonCommercial 4.0 International (CC BY-NC 4.0 license) (<http://creativecommons.org/licenses/by-nc/4.0/>).

How to cite this article: Pourabdy M., Shishehsaz M., Shahrooi S., Roknizadeh S.A.S. Analysis of Axisymmetric Vibration of Functionally-Graded Circular Nano-Plate Based on the Integral Form of the Strain Gradient Model, *J. Appl. Comput. Mech.*, 7(4), 2021, 2196–2220. <https://doi.org/10.22055/JACM.2021.37461.3021>

Publisher's Note Shahid Chamran University of Ahvaz remains neutral with regard to jurisdictional claims in published maps and institutional affiliations.

